Quantifying macro-evolutionary patterns of trait mean and variance with phylogenetic location-scale models

Shinichi Nakagawa[1,2,*], Ayumi Mizuno[1], Coralie Williams[2,3], Malgorzata Lagisz[1,2], Yefeng Yang[2], and Szymon M Drobniak[2,4]

[1]Department of Biological Sciences, Faculty of Science, University of Alberta, Edmonton, Canada
[2]Evolution and Ecology Research Centre, School of Biological, Earth and Environmental Sciences, University of New South Wales, Sydney, New South Wales, Australia
[3]School of Mathematics and Statistics, The University of New South Wales, Sydney, New South Wales, Australia
[4]Institute of Environmental Sciences Jagiellonian University, Kraków, Poland
[*]snakagaw@ualberta.ca / s.nakagawa@unsw.edu.au

September 10, 2025

Running head: Phylogenetic location-scale model

Author Statement

Conceptualization: Shinichi Nakagawa, Szymon M Drobniak. Data curation: Shinichi Nakagawa, Ayumi Mizuno. Formal analysis: Shinichi Nakagawa, Szymon M Drobniak. Funding Acquisition: Shinichi Nakagawa, Malgorzata Lagisz. Investigation: Shinichi Nakagawa. Methodology: Shinichi Nakagawa, Ayumi Mizuno, Szymon M Drobniak. Project administration & Supervision: Shinichi Nakagawa. Validation: Szymon M Drobniak, Ayumi Mizuno, Yefeng Yang, Coralie Williams. Visualization: Szymon M Drobniak, Ayumi Mizuno, Shinichi Nakagawa. Writing - Original Draft: Shinichi Nakagawa. Writing - Review & Editing: All authors.

Data Availability Statement

All data, scripts and relevant files used for this study can be found at the GitHub repository (link), and a version of it has been archived at Zenodo (link).

Acknowledgments

SN and AM were supported by a Canada Excellence Research Chair (CERC-2022-00074). Also, YY, SN, and ML were supported by an Australian Research Council Discovery Grant (DP230101248).

Abstract

1. Understanding how both the mean (*location*) and variance (*scale*) of traits differ among species and lineages is fundamental to unveiling macroevolutionary patterns. Yet, traditional phylogenetic comparative methods primarily focus on modelling mean trait values, often overlooking variability and heteroscedasticity that can provide critical insights into evolutionary dynamics.
2. Here, we introduce phylogenetic location-scale models (PLSMs), a novel framework that jointly analyses the evolution of trait means and variances. This dual approach captures heteroscedasticity and evolutionary changes in trait variability, allowing for the detection of clades with differing variances and revealing patterns of adaptation, diversification, and evolutionary constraints.
3. Extending PLSMs to a multivariate context enables simultaneous analysis of multiple traits and their covariances, facilitating the testing of hypotheses about evolutionary trade-offs, pleiotropy, and phenotypic integration. By modelling covariances between phylogenetic effects in both the *location* and *scale* parts, we can discern whether changes in one trait's mean or variance are associated with changes in another's, thereby offering deeper insights into the mechanisms driving trait co-evolution, and co-divergence or "contra-divergence".
4. We also describe how an extended version of PLSMs incorporating within-species variability can enhance our understanding of trait convergence and divergence arising from ecological and environmental factors.
5. Our framework provides a powerful tool for exploring macroevolutionary patterns and can be used to reassess previously published comparative data, offering new insights into the mechanisms driving the diversity of life.

Keywords— phylogenetic comparative method, double-hierarchical model, phylogenetic generalised least squares, phylogenetic generalised linear mixed-effects model, Bayesian statistics

1 Introduction

Understanding how traits evolve across species is a central theme in evolutionary biology. Phylogenetic comparative methods (PCMs), particularly regression-based approaches, have played a pivotal role in revealing patterns of trait evolution by accounting for shared ancestry among species (Felsenstein, 1985; Garland and Ives, 2000; Cornwallis and Griffin, 2024). Traditional methods, such as phylogenetically independent contrasts (PICs) and phylogenetic generalised least squares (PGLS), have focused on modelling mean trait values, shedding light on average evolutionary trends (Hansen and Martins, 1996). However, these approaches often assume homogeneity in trait variance (i.e., homoscedasticity) across species and lineages, potentially missing key aspects of macro-evolutionary processes tied to variability and dispersion (e.g., Cleasby and Nakagawa, 2011).

Contrary to the common assumption that selection acts solely on trait means, evidence suggests that trait variance itself can be subject to selection. For instance, dairy cows can be selectively bred for reduced variability in milk production, or pigs can be bred for producing similar litter sizes, demonstrating that genetic mechanisms can influence trait variance in addition to means (Mulder et al., 2008). Further, earlier work supports that variance and covariance structures evolve. Theoretically and empirically, genetic variances and covariances ($\mathbf{G}$) can change through time as selection and mutation–drift regimes shift (Turelli, 1984, 1988; Shaw et al., 1995). Across species, phenotypic integration and modularity studies show that the pattern of trait covariation ($\mathbf{P}$) differs among clades (Porto et al., 2009; Marroig et al., 2009; Haber, 2016). Importantly for macroevolution, comparative methods have detected heterogeneity in evolutionary covariances among regimes or clades (Revell and Collar, 2009; Hermansen et al., 2018). These findings point to the need for comparative models that treat (co)variances as evolvable quantities, not fixed background noise (Bruijning et al., 2020).

Indeed, patterns of trait (co)variance can reveal critical insights into macro-evolutionary dynamics, such as release from stabilising selection, adaptive radiation, or transitions to evolutionary optima (Hansen et al., 2008). For example, a positive correlation between species' mean and variance within a trait in a clade may indicate a release from selection, allowing greater phenotypic diversity; in other words, a shift in mean trait values leads to increased trait variation within a clade. Conversely, changes in the mean accompanied by a reduction in variance could signify the attainment of an adaptive peak or the presence of biological constraints limiting further diversification. As indicated in earlier studies, mentioned above, particular clades may harbour more variance in specific traits due to ecological opportunities or historical contingencies. However, direct investigations of variance are extremely rare in macro-evolutionary studies. This is probably because the different patterns of variance can arise due to two distinct processes: (1) the selection of trait means, resulting in changes in population variance, and (2) selection on trait variance, also resulting in similar changes (cf. Hill and Mulder, 2010; Mulder et al., 2008). Macro-evolutionary research seemed to have focused on the former but not the latter (e.g., stabilising selection is seen as a byproduct of selection on means rather than direct selection on variance).

Importantly, following the Brownian motion model of evolution, the mean and the variance of a quantitative trait could diffuse independently on a phylogeny, because each is governed by its own mutational (or developmental) input and can experience separate selective pressures (Turelli, 1984; Wagner et al., 2008). In quantitative-genetic terms, a trait's expected value evolves under one Brownian process with rate σ^2_μ, whereas the log of its residual (within-lineage/among species unexplained) variance can evolve under a second, independent process with rate $\sigma^2_{\ln(\sigma^2)}$ (Hill and Mulder, 2010; Mulder et al., 2008). Empirical evidence for such dual diffusion comes from clade-wide heterogeneity in canalisation, bet-hedging, and evolvability statistics (Hansen and Houle, 2008). Consequently, treating variance as an evolvable character alongside the mean is not only biologically plausible but mathematically consistent with the standard comparative framework; failing to model it risks conflating two distinct evolutionary signals.

Incorporating both the mean (*location*) and the residual variance (*scale*) offers a more complete view of macro-evolutionary dynamics, because evolutionary processes can reshape not only the average phenotype but also dispersion (cf. Hunt, 2007). Rapid mean shifts, for example during adaptive radiations, are often accompanied by increased among-lineage variance, yet such joint patterns are rarely analysed within a single framework (see Fig. 1). Here we extend the phylogenetic generalised linear mixed-model (PGLMM) framework (Lynch, 1991; Hadfield and Nakagawa, 2010; Ives and Helmus, 2011) by introducing *phylogenetic location-scale models* (PLSMs). A PLSM treats the mean and the log-variance (standard deviation) as parallel response variables, each with its own fixed effects and phylogenetic random effect, thereby quantifying the co-evolution of trait means and variances (Lee and Nelder, 1996, 2006; Cleasby et al., 2015). Notably, some related approaches, such as the "Fabric" model (Pagel et al., 2022; Pagel and Meade, 2025), allow evolutionary rates (parting to variation due to phylogeny) to vary discretely across the phylogeny, identifying branches where directional trends and rate parameters shift. Instead, our approach allows us to test whether particular clades harbour unusually high heteroscedasticity, whether mean–variance correlations signal evolutionary limits or trade-offs, and, via a multivariate extension, whether two traits show mean–mean, variance–variance, or mean–variance co-evolution (Fig. 2). Throughout, we show how PLSMs capture evolutionary changes in trait variability that conventional PCMs overlook.

Below, we develop PLSMs in four steps (cf. Halliwell, 2025). First, we describe the statistical framework of PLSMs, starting with a model without a random effect in the *scale* part and introducing relevant concepts such as phylogenetic heritability (Lynch, 1991) and evolvability (Houle, 1992). Second, we extend this PLSM to include phylogenetic effects in both the *location* and *scale* components. Third, we generalise the model to a multivariate context, enabling the simultaneous analysis of multiple traits and their covariances. Fourth, we incorporate within-species variation into PLSMs, allowing individual-level measurements to be accommodated. This model allows us to gain insights into trait convergence or divergence due to ecological and environmental factors by quantifying both non-phylogenetic and phylogenetic effects (throughout the paper, we designate within-species variation as ε and among-species residual variation as e; only the latter is modelled by the scale component unless individual data are available). We then discuss how patterns of variance evolution can inform macro-evolutionary processes such as adaptive radiation and release from selection, and demonstrate the applicability of our model through empirical examples. Notably, this paper includes an online tutorial (link) to help implement the PLSMs introduced here using `brms` (Bürkner, 2017) in R.

2 Developing Phylogenetic Location-Scale Models (PLSMs)

Before diving into mathematical definitions of phylogenetic location-scale models (PLSMs), it may be useful to have an overview of key variables and parameters in PLSMs, summarised in Table 1. This table provides biological interpretations of each notation. Also, for many readers, it may be helpful to look at the `brms` code snippets corresponding to the formulas (equations) below in our online tutorial.

2.1 PLSMs without the Phylogenetic Effect on the *Scale* Part

A phylogenetic location-scale model has two parts: 1) the *location* (mean) part and 2) the *scale* (variance) part; the simple example of such a model can be written as (Model 1):

$$y_i = \beta_0^{(l)} + a_i^{(l)} + e_i^{(l)}, \tag{1}$$

$$\{a_i\} = \mathbf{a} \sim \mathcal{N}(\mathbf{0}, \sigma^2_{a(l)}\mathbf{A}), \tag{2}$$

$$\{e_i^{(l)}\} = \mathbf{e}^{(l)} \sim \mathcal{N}\left(\mathbf{0}, \sigma^2_{e_i(l)}\mathbf{I}\right), \tag{3}$$

$$\ln\left(\sigma_{e_i(l)}\right) = \beta_0^{(s)}, \tag{4}$$

where y_i is the observed trait value for species i, $\beta_0^{(l)}$ denotes the intercept term in the *location* part of the model, representing the overall mean trait value across all species. The term $a_i^{(l)}$ is the phylogenetic effect for species i in the location part, capturing the variation due to shared evolutionary history among species. As specified in Equation 2, these phylogenetic effects (a_i or the vector $\mathbf{a}$) are assumed to follow a multivariate normal distribution with mean zero and covariance structure $\sigma^2_{a(l)}\mathbf{A}$, where $\sigma^2_{a(l)}$ is the variance component associated with the phylogenetic effects, and $\mathbf{A}$ is the phylogenetic correlation matrix derived from an ultrametric phylogenetic tree so containing information on species relatedness (a correlation matrix is only calculable when a phylogenetic tree is ultrametric). The residual error term $e_i^{(l)}$ (or the vector $\mathbf{e}^{(l)}$) in the location part, as shown in Equation 3, accounts for the unexplained variation in trait values after accounting for phylogenetic effects. These residuals are assumed to be independently and normally distributed with mean zero and species-specific variance $\sigma^2_{e_i(l)}$, and $\mathbf{I}$ is the identity matrix (a diagonal matrix of 1's).

The *scale* (variance) part of the model is given in Equation 4, where the natural logarithm of the residual standard deviation σ_{e_i} is modelled as a constant intercept $\beta_0^{(s)}$ on the *scale* part; note that the *scale* part could take either the residual standard deviation or residual variance, which is a matter of preference; for an example of using residual variance (see O'Dea et al., 2022). This implies that the residual variances are homoscedastic across species unless extended to include additional predictors or random effects. By modelling the logarithm of the residual standard deviation, we ensure that the estimated variances are positive, but we acknowledge that variability in trait measurements may differ across species, which is yet to be modelled (see below). Also, it is important to note that Equation 3 is equivalent to $e_i^{(l)} \sim \mathcal{N}\left(\mathbf{0}, \sigma_e^2\mathbf{I}\right)$. The variance component σ_e^2 is often considered to be the non-phylogenetic effect, which consists of species variation not due to shared phylogenetic history (assuming measurement errors are negligible in y_i and y_i is a representative measurement for species i, e.g., species mean so that y_i does not include within-species variation; for modelling within-species variance, see Section 2.4).

Before building upon this basic formulation, we introduce two key concepts in phylogenetic comparative methods (PCMs). The first one is phylogenetic heritability, introduced by Lynch (1991). Phylogenetic heritability (denoted as $H^2_{(l)}$) is the ratio between the phylogenetic variance and the sum of the phylogenetic and residual variance, showing the amount of "phylogenetic signal", which is often quantified by Pagel's λ (Pagel, 1999). Although Housworth et al. (2004) state Pagel's λ and phylogenetic heritability are equivalent, Pearse et al. (2025) have recently pointed out that this cannot be the case. This is because Pagel's λ can exceed one while phylogenetic heritability $H^2_{(l)}$ cannot although both are closely related:

$$H^2_{(l)} = \frac{\sigma^2_{a(l)}}{\sigma^2_{a(l)} + \overline{\sigma^2}_{e(l)}}, \tag{5}$$

where $\overline{\sigma^2}_{e(l)}$ is the expected (average) value of $\sigma^2_{e_i(l)}$ or it is equivalent to $\exp\left(\beta_0^{(s)}\right)^2$ for the model above.

The other is evolvability, proposed by Houle (1992); evolvability is the additive genetic standard deviation, divided by the expected (average) value of a trait. An analogous quantity can be obtained as follows:

$$CV_{A(l)} = \frac{\sigma_{a(l)}}{\beta_0^{(l)}}, \tag{6}$$

where CV denotes the coefficient of variation, which is a popular mean-standardised dispersion measure. We can call this quantity "macro-evolvability" while the original evolvability can be referred to as "micro-evolvability" as with macro- and micro-evolution. Macro-evolvability values indicate the potential for a given trait to evolve and, like phylogenetic heritability, are supposed to be comparable across traits (later, we expand these two concepts to the *scale* part; note that for estimating parameters in these indexes, we use estimators such as Bayesian MCMC estimators). We note that $CV_{A(l)}$ can sometimes be more involved to obtain, as we usually ln-transform trait values, and then, we need to convert such values back into the original scale. This is because CV is usually only calculable on the original scale, which is the ratio scale where measurements are all above zero (for example, see our online tutorial; see also O'Dea et al., 2022). However, for ratio-scale traits (i.e., $y > 0$), there is a simple connection between dispersion on the original and log scales. If y is log-normal distributed, SD on the natural log scale ($\ln y$ is approximately CV on the original scale, when CV < 0.3 (Lynch, 1990). This equivalence is useful as many continuous traits are on the ratio scale; also, such traits should usually be ln-transformed for analysis.

We can now add predictors to both parts of Model 1 to generalise (Model 2):

$$y_i = \beta_0^{(l)} + \sum_{k=1}^{K} \beta_k^{(l)} x_{ki} + a_i^{(l)} + e_i^{(l)} \tag{7}$$

$$\ln(\sigma_{e_i(l)}) = \beta_0^{(s)} + \sum_{k=1}^{K} \beta_k^{(s)} x_{ki} \tag{8}$$

where x_{ki} is the value of the k-th predictor variable for species i; $\beta_k^{(l)}$ are the coefficients associated with the predictors in the *location* part, representing the effect of each predictor x_{ki} on the mean trait value; and $\beta_k^{(s)}$ are the coefficients in the *scale* part, capturing how each predictor x_{ki} influences the logarithm of the residual standard deviation σ_{e_i} (with with $k = 1, 2...K$). By incorporating predictors into both parts of the model, we allow for the possibility that explanatory variables affect not only the mean trait values but also the variance, enabling a more comprehensive understanding of the factors influencing trait evolution.

To show the usefulness of this type of PSLMs and make it more concrete, consider a scenario where we are interested in the evolution of brain size (y) across two classes of vertebrates (e.g., birds and mammals). We hypothesise that, after controlling for body size (x_1), two different vertebrate classes (x_2, a dummy variable) have different variances (i.e., heteroscedasticity). Then, we may have the following model (Model 3):

$$y_i = \beta_0^{(l)} + \beta_1^{(l)} x_{1i} + \beta_2^{(l)} x_{2i} + a_i^{(l)} + e_i^{(l)}, \tag{9}$$

$$\ln(\sigma_{e_i(l)}) = \beta_0^{(s)} + \beta_1^{(s)} x_{1i} + \beta_2^{(s)} x_{2i}, \tag{10}$$

where a significant $\beta_1^{(s)}$ indicates changes in variance along body size while a significant $\beta_2^{(s)}$ indicates different variances between two groups (note that depending on your questions, you may decide to model the interaction between body size and vertebrate classes (x_1 and x_2), and also we do not necessarily have to have the same predictors in both parts of the model; e.g., not having body size in the *scale* part) and two classes (x_2). Yet, without clear hypotheses, the same fixed effects in both parts could be fitted. Model 3 and related models are useful for detecting which clades have more variation in a given trait. Relatively high variance in a clade may represent relaxed selection or adaptations to diverse niches, while low variance could mean strong stabilising selection (i.e., the existence of trait optima; Fig 3).

2.2 PLSMs with the Phylogenetic Effect on the *Scale* Part

Although the above models (Models 1-3) are useful first steps to model mean and variance simultaneously, they cannot tell us whether mean and variance are co-evolving in a trait across species. To model such an effect, we will need the following model extending the *scale* part of Model 3 (Model 4; note its *mean* part is Equation 7):

$$\ln(\sigma_{e_i(l)}) = \beta_0^{(s)} + \sum_{k=1}^{K} \beta_k^{(s)} x_{ki} + a_i^{(s)}, \tag{11}$$

$$\begin{pmatrix} a_i^{(l)} \\ a_i^{(s)} \end{pmatrix} \sim \mathcal{N}\left(\mathbf{0}, \mathbf{\Sigma}_a \otimes \mathbf{A}\right), \tag{12}$$

where $a_i^{(s)}$ is the phylogenetic effect in the *scale* part, capturing the phylogenetic variation in residual variances among species. The vector of phylogenetic effects $(a_i^{(l)},\ a_i^{(s)})'$ follows a multivariate normal distribution with mean zero and $\mathbf{\Sigma}_a \otimes \mathbf{A}$, which is:

$$\mathbf{\Sigma}_a \otimes \mathbf{A} = \begin{pmatrix} \sigma^2_{a(l)}\mathbf{A} & \rho_{a(ls)}\sigma_{a(l)}\sigma_{a(s)}\mathbf{A} \\ \rho_{a(ls)}\sigma_{a(l)}\sigma_{a(s)}\mathbf{A} & \sigma^2_{a(s)}\mathbf{A} \end{pmatrix}, \tag{13}$$

with $\sigma^2_{a(l)}$ and $\sigma^2_{a(s)}$ representing the phylogenetic variances for the *location* and *scale* parts, respectively, and $\rho_{a(ls)}$ denoting the correlation between the phylogenetic effects in the two parts. The operator $\otimes$ denotes the Kronecker product, indicating that the covariance matrix is constructed by multiplying the variance-covariance matrix $\mathbf{\Sigma}_a$ with the phylogenetic correlation matrix $\mathbf{A}$.

By incorporating the phylogenetic effect $a_i^{(s)}$ in the *scale* part and allowing for a correlation $\rho_{a(ls)}$ between $a_i^{(l)}$ and $a_i^{(s)}$, Model 4 enables us to investigate whether the mean and variance of the trait are co-evolving across species due to shared ancestry. A significant correlation $\rho_{a(ls)}$ suggests that species with higher (or lower) mean trait values also tend to have higher (or lower) trait variability, which may reflect evolutionary processes affecting both the mean and variance of the trait. For example, we may get a negative $\rho_{a(ls)}$ (e.g., larger traits are associated with lower variance), and such a correlation value could indicate the existence of a ceiling or optimal trait value for a clade (Fig 2).

Given Model 4, we redefine phylogenetic heritability for the *location* part, which is more general than Equation 5:

$$H^2_{(l)} = \frac{\sigma^2_{a(l)}}{\sigma^2_p}, \tag{14}$$

where σ^2_p is the observed phenotypic (trait) variance, calculated as the sum of the variance components from the fixed effects, phylogenetic effects, and residual variance (i.e., all the elements in the model):

$$\sigma^2_p = \sigma^2_{f(l)} + \sigma^2_{a(l)} + \overline{\sigma^2}_{e(l)}. \tag{15}$$

In this expression, $\sigma^2_{f(l)}$ represents the variance due to fixed effects in the *location* part, computed as (Nakagawa and Schielzeth, 2013):

$$\sigma^2_{f(l)} = \mathrm{Var}\left(\sum_{k=1}^{K} \beta_k^{(l)} x_{ki}\right), \tag{16}$$

and $\overline{\sigma^2}_{e_i(l)}$ is the average residual variance across species in the *location* part, given by (O'Dea et al., 2022):

$$\overline{\sigma^2}_{e(l)} = \exp\left(2\beta_0^{(s)} + 2\sigma^2_{a(s)}\right). \tag{17}$$

Similarly, we can define phylogenetic heritability for the *scale* part:

$$H^2_{(s)} = \frac{\sigma^{*2}_{a(s)}}{\sigma^2_{\sigma^2_p}}. \tag{18}$$

Since the *scale* part is on the natural log scale, we need to back-transform $\sigma^2_{a(s)}$ to the original scale (or the same scale as in the *location* part) to obtain $\sigma^{*2}_{a(s)}$ (following Hill and Mulder, 2010; Mulder et al., 2016):

$$\sigma^{*2}_{a(s)} = \sigma^2_{\sigma^2_{e(l)}} \left(\frac{\sigma^2_{a(s)}}{\sigma^2_{a(s)} + \sigma^2_{f(s)}}\right). \tag{19}$$

Here, $\sigma^2_{\sigma^2_p}$ is the variance of the phenotypic variance σ^2_p, calculated as (Hill and Mulder, 2010; Mulder et al., 2016):

$$\sigma^2_{\sigma^2_p} = 2\sigma^4_p + 3\sigma^2_{\sigma^2_{e(l)}}. \tag{20}$$

In this context, $\sigma^2_{\sigma^2_{e(l)}}$ is the variance of the residual variances in the *location* part, expressed as:

$$\sigma^2_{\sigma^2_{e(l)}} = \left(\exp\left(4\left(\sigma^2_{a(s)} + \sigma^2_{f(s)}\right)\right) - 1\right) \exp\left(4\left(\beta_0^{(s)} + \sigma^2_{a(s)} + \sigma^2_{f(s)},\right)\right) \tag{21}$$

and $\sigma^2_{f(s)}$ represents the variance due to fixed effects in the *scale* part, computed as:

$$\sigma^2_{f(s)} = \operatorname{Var}\left(\sum_{k=1}^{K} \beta_k^{(s)} x_{ki}\right). \tag{22}$$

For macro-evolvability, we use Equation 6 for the *location* part and for the *scale* part, macro-evolvability is defined as:

$$CV_{A(s)} = \frac{\sigma^*_{a(s)}}{\overline{\sigma^2}_{e(l)}}. \tag{23}$$

An alternative expression for $CV_{A(s)}$ which is applicable if $a_i^{(s)}$ is the only random effect in the *scale* part (also, this is easier as we do not need to transform back $\sigma^2_{a(s)}$)—is (for the derivation from Equation 23, O'Dea et al., 2022):

$$CV_{A(s)} = \sqrt{\exp(4\sigma^2_{a(s)}) - 1}. \tag{24}$$

Earlier relevant papers from quantitative genetics – where mixed-effects models and associated location-scale models are initially developed – indicate phylogenetic heritability values on the *scale* part ($H^2_{(s)}$) may be informative yet tend to be small, compared to that of the location part (Hill and Mulder, 2010; Mulder et al., 2016; Sae-Lim et al., 2015; O'Dea et al., 2022). However, the macro-evolvability values for the scale part may remain relatively high compared to those for the location part ($H^2_{(l)}$). So, estimating evolvability for location and scale parts may be useful under some circumstances. Notably, macro-evolvability values can be challenging to obtain, as it is not clear on what scale evolvability should be calculated, and it seems to be only meaningful when traits are on ratio scale (e.g., or example that the median macro-evolvability on the original scale was 0.38 while on the log scale this is 0.83, as we have shown in the online tutorial). Furthermore, to add to the complexity, although we introduce the CV for variance (Equation 24), it may be better to have the CV for standard deviation (SD) because mean and SD are on the same scale. In such a case, we have (Cleasby et al., 2015):

$$CV^*_{A(s)} = \sqrt{\exp(\sigma^2_{a(s)}) - 1}. \tag{25}$$

2.3 Multivariate (Multi-Response) PLSMs

So far, we have focused on the evolution of a single trait; however, traits often evolve in conjunction with others due to genetic, developmental, or functional linkages. To capture these relationships, we need to extend our models to accommodate multiple traits simultaneously (**?**). Multivariate or multi-response PLSMs allow us to model the evolution of several traits and their covariances, providing a more comprehensive understanding of the evolutionary processes at play.

In the simplest case of a bi-variate PLSM, we consider two traits, $y^{(1)}$ (trait 1) and $y^{(2)}$ (trait 2), across species. Such a bi-variate model can be expressed as (Model 5):

$$\mathbf{y}_i = \begin{pmatrix} y_i^{(1)} = \beta_0^{(l1)} + \sum_{k=1}^{K} \beta_k^{(l1)} x_{ki} + a_i^{(l1)} + e_i^{(l1)} \\ y_i^{(2)} = \beta_0^{(l2)} + \sum_{k=1}^{K} \beta_k^{(l2)} x_{ki} + a_i^{(l2)} + e_i^{(l2)} \end{pmatrix}, \tag{26}$$

$$\mathbf{s}_i = \begin{pmatrix} \ln(\sigma_{e_{i(l1)}}) = \beta_0^{(s1)} + \sum_{k=1}^{K} \beta_k^{(s1)} x_{ki} + a_i^{(s1)} \\ \ln(\sigma_{e_{i(l2)}}) = \beta_0^{(s2)} + \sum_{k=1}^{K} \beta_k^{(s2)} x_{ki} + a_i^{(s2)} \end{pmatrix}. \tag{27}$$

In these equations, the vector $\mathbf{y}_i$ (length of 2) represents a set of two trait values for species i while the vector $\mathbf{s}_i$ is a set of two residual standard deviations on the natural logarithm scale. The coefficients $\beta_0^{(l1)}$, $\beta_0^{(l2)}$, $\beta_k^{(l1)}$, and $\beta_k^{(l2)}$ are the intercept and predictor effects for trait 1 and 2 in the *location* part, while $\beta_0^{(s1)}$, $\beta_0^{(s2)}$, $\beta_k^{(s1)}$, and $\beta_k^{(s2)}$ are the corresponding parameters in the *scale* part. The terms $a_i^{(l1)}$, $a_i^{(l2)}$, $a_i^{(s1)}$, and $a_i^{(s2)}$ are the phylogenetic effects for species i in the *location* and *scale* parts of trait 1 and 2, respectively, capturing the shared evolutionary history.

The vector of phylogenetic effects for both traits and both parts is jointly modelled to account for correlations between traits and between the mean and variance. Specifically, the random effects are assumed to follow a multivariate normal distribution:

$$\begin{pmatrix} a_i^{(l1)} \\ a_i^{(l2)} \\ a_i^{(s1)} \\ a_i^{(s2)} \end{pmatrix} \sim \mathcal{N}\left(\begin{pmatrix} 0 \\ 0 \\ 0 \\ 0 \end{pmatrix}, \mathbf{\Sigma}_a \otimes \mathbf{A} \right), \tag{28}$$

$$\mathbf{\Sigma}_a = \begin{pmatrix} \sigma^2_{a(l1)} & \rho_{a(l1l2)}\sigma_{a(l1)}\sigma_{a(l2)} & \rho_{a(l1s1)}\sigma_{a(l1)}\sigma_{a(s1)} & \rho_{a(l1s2)}\sigma_{a(l1)}\sigma_{a(s2)} \\ \rho_{a(l1l2)}\sigma_{a(l1)}\sigma_{a(l2)} & \sigma^2_{a(l2)} & \rho_{a(l2s1)}\sigma_{a(l2)}\sigma_{a(s1)} & \rho_{a(l2s2)}\sigma_{a(l2)}\sigma_{a(s2)} \\ \rho_{a(l1s1)}\sigma_{a(l1)}\sigma_{a(s1)} & \rho_{a(l2s1)}\sigma_{a(l2)}\sigma_{a(s1)} & \sigma^2_{a(s1)} & \rho_{a(s1s2)}\sigma_{a(s1)}\sigma_{a(s2)} \\ \rho_{a(l1s2)}\sigma_{a(l1)}\sigma_{a(s2)} & \rho_{a(l2s2)}\sigma_{a(l2)}\sigma_{a(s2)} & \rho_{a(s1s2)}\sigma_{a(s1)}\sigma_{a(s2)} & \sigma^2_{a(s2)} \end{pmatrix}. \tag{29}$$

where $\mathbf{A}$ is the phylogenetic correlation matrix, and $\mathbf{\Sigma}_a$ is the variance-covariance matrix of the phylogenetic effects.

Here, $\sigma^2_{a(l1)}$, $\sigma^2_{a(l2)}$, $\sigma^2_{a(s1)}$ and $\sigma^2_{a(s2)}$ are the phylogenetic variances for the *location* and *scale* parts of trait 1 and 2, respectively. The terms $\rho_{a(l1l2)}$, $\rho_{a(s1s2)}$, $\rho_{a(l1,s1)}$, $\rho_{a(l2\,s2)}$, $\rho_{a(l1\,s2)}$, and $\rho_{a(l2s1)}$ represent the correlations between the phylogenetic effects, capturing various types of coevolutionary relationships. Specifically, $\rho_{a(l1l2)}$ reflects across-trait mean-mean coevolution, indicating whether evolutionary changes in the mean of one trait are associated with changes in the mean of another trait due to shared ancestry (i.e., coevolution of traits). For example, a positive correlation may mean pleiotropy (the same set of genes affecting two traits in the same manner) and phenotypic integration (e.g., coevolution of wing and muscle size in birds; cf., Pigliucci, 2003), whereas a negative correlation could represent an evolutionary trade-off.

The term $\rho_{a(s1s2)}$ represents across-trait variance-variance coevolut ion, indicating whether the variability in one trait is evolutionarily linked to the variability in another trait; this is a new insight obtained from Model 5. Positive $\rho_{a(s1s2)}$ can also indicate pleiotropy (given a set of genes that affect a trait variability; see Mulder et al. 2008) and phenotypic integration, which we call "co-divergence". In contrast, negative $\rho_{a(s1s2)}$ could show a trade-off; a famous yet statistically untested example is that avian lineages in which increased variability in male songs are often accompanied by reduced variation in male plumage. Such negative correlations can be called "contra-divergence". Furthermore, it can suggest relaxed selection and adaptations to different environments for a set of two traits in a clade (see Fig 2). However, phylogenetic variance on the *scale* part (i.e., $\sigma^2_{a(s)}$) can be confounded by external factors if we have missing predictors, which pertain to trait variability. Given that one is unlikely to have all the information about a trait, one needs to exercise caution in interpreting $\rho_{a(s1s2)}$ or any quantities involving $\sigma^2_{a(s)}$. This issue is somewhat reduced once we have multiple data points per species, which will be described in the next sub-section.

The correlations $\rho_{a(l1s1)}$ and $\rho_{a(l2s2)}$ denote within-trait mean-variance coevolution, showing whether species with higher (or lower) mean trait values also tend to have higher (or lower) variability in the same trait (Model 4 can provide such correlations for one trait). Lastly, $\rho_{a(l1s2)}$ and $\rho_{a(l2s1)}$ capture across-trait mean-variance coevolution, examining whether the mean of one trait is evolutionarily associated with the variance of another trait. At first glance, it is hard to imagine the evolutionary significance of such correlations ($\rho_{a(l1s2)}$ and $\rho_{a(l2s1)}$). Yet, such a correlation can signify that, for example, a shift in mean in trait 1 can relax selection in trait 2 (an increase in variance in trait 2), therefore, they are evolutionarily meaningful.

The residual errors for the *location* parts are also allowed to be correlated across traits:

$$\begin{pmatrix} e_i^{(l1)} \\ e_i^{(l2)} \end{pmatrix} \sim \mathcal{N}\left(\begin{pmatrix} 0 \\ 0 \end{pmatrix}, \mathbf{\Sigma}_e \otimes \mathbf{I}\right), \tag{30}$$

$$\mathbf{\Sigma}_e = \begin{pmatrix} \sigma^2_{e(l1)} & \rho_{e(l1l2)}\sigma_{e(l1)}\sigma_{e(l2)} \\ \rho_{e(l1l2)}\sigma_{e(l1)}\sigma_{e(l2)} & \sigma^2_{e(l2)} \end{pmatrix}, \tag{31}$$

where $\sigma^2_{e(l1)}$ and $\sigma^2_{e(l2)}$ are the residual variance for the *location* part of trait 1 and, and $\rho_{e(l1l2)}$ is the correlation between the residual errors of the two traits in the *location* part.

This multivariate PLSM allows us to explore not only how each trait evolves individually but also how their means and variances coevolve. By modelling the covariance structures, we can test hypotheses about evolutionary trade-offs, pleiotropy, and adaptive diversification. For instance, a significant positive $\rho_{a(l1l2)}$ would indicate that species with higher mean values in trait 1 also tend to have higher mean values in trait 2 due to shared evolutionary history. Quantifying a set of these four different types of phylogenetic correlations provides exciting avenues to discover and test different evolutionary patterns.

The bivariate model can be extended to more than two traits, leading to a multivariate PLSM. In matrix notation, the *location* part and and the *scale* part of the model for species i becomes, respectively (Model 6):

$$\mathbf{y}_i = \mathbf{X}_i\boldsymbol{\beta}^{(l)} + \mathbf{a}_i^{(l)} + \mathbf{e}_i^{(l)}, \tag{32}$$

$$\mathbf{s}_i = \ln\left(\boldsymbol{\sigma}_{e_{i(l)}}\right) = \mathbf{X}_i\boldsymbol{\beta}^{(s)} + \mathbf{a}_i^{(s)}, \tag{33}$$

where $\mathbf{y}_i$ is a vector of trait values for species i while $\mathbf{s}_i$ is a vector of residual standard deviation values on the natural logarithm scale, $\mathbf{X}_i$ is the design matrix of predictors, $\boldsymbol{\beta}^{(l)}$ and $\boldsymbol{\beta}^{(s)}$ are vectors of coefficients for the *location* and *scale* parts, and $\mathbf{a}_i^{(l)}$ and $\mathbf{a}_i^{(s)}$ are vectors of phylogenetic effects for the *location* and *scale* parts, respectively. The residual errors $\mathbf{e}_i^{(l)}$ are assumed to follow a multivariate normal distribution with appropriate covariance structure.

Expanding the model to multiple traits increases the complexity of the covariance matrices, but the fundamental approach remains the same. By modelling the covariances among multiple traits in both the mean and variance components, we can gain a deeper understanding of the evolutionary dynamics shaping trait evolution by obtaining the four types of phylogenetic correlations: 1) across-trait mean-mean, 2) across-trait variance-variance, 3) within-trait mean-variance and 4) across-trait mean-variance phylogenetic correlation. This comprehensive approach enhances our ability to detect patterns such as evolutionary constraints, correlated responses to selection, and the potential for adaptive diversification across multiple traits.

2.4 PLSMs with Non-Phylogenetic Effects and Within-Species Variation

In the previous sections, we have considered models where each species is represented by a single observation (a representative value per species). However, in empirical studies, multiple measurements are taken from individuals within species, providing within-species variation. Incorporating within-species variation allows us to partition the phenotypic variance into phylogenetic effects, species-specific non-phylogenetic effects, and individual-level residuals (cf. Rohlfs et al., 2014; Silvestro et al., 2015; Gaboriau et al., 2020). To accommodate this, we extend the PLSM framework by including additional random effects at the species level that are not phylogenetically structured, as well as individual-level residuals.

The extended model is formulated as (Model 7):

$$y_{ij} = \beta_0^{(l)} + \sum_{k=1}^{K} \beta_k^{(l)} x_{kij} + a_i^{(l)} + e_i^{(l)} + \varepsilon_{ij}^{(l)}, \tag{34}$$

$$\ln\left(\sigma_{\varepsilon_{ij(l)}}\right) = \beta_0^{(s)} + \sum_{k=1}^{K} \beta_k^{(s)} x_{kij} + a_i^{(s)} + e_i^{(s)}, \tag{35}$$

$$\varepsilon_{ij}^{(l)} \sim \mathcal{N}\left(0, \sigma^2_{\varepsilon_{ij(l)}}\right), \tag{36}$$

where y_{ij} is the observed trait value for the j-th individual in species i, and x_{kij} represents the value of the k-th predictor variable for that individual (note that Model 7 can have two types of fixed factors: individual-level predictors e.g., sex of birds and species-level predictors, e.g., mating systems of species). The term $\beta_0^{(l)}$ is the intercept in the *location* part, while $\beta_k^{(l)}$ are the coefficients for the predictors in the *location* part. The phylogenetic effect $a_i^{(l)}$ accounts for the shared evolutionary history among species in the mean trait values. The species-specific non-phylogenetic effect $e_i^{(l)}$ captures additional variation at the species level that is not explained by phylogeny. The individual-level residual error $\varepsilon_{ij}^{(l)}$ represents within-species variation, assumed to follow a normal distribution with mean zero and variance $\sigma^2_{\varepsilon_{ij(l)}}$, which may vary among individuals. The term $\beta_0^{(s)}$ and $\beta_k^{(s)}$ are the intercept and coefficients in the *scale* part, respectively. The phylogenetic effect $a_i^{(s)}$ captures the phylogenetic variation in the residual variances among species, while $e_i^{(s)}$ is a species-specific non-phylogenetic effect in the *scale* part. It is important to clarify that the residual term $\varepsilon_{ij}^{(l)}$ represents something very different from the residual term ($e_i^{(l)}$) in Equation 3. The former relates to within-species variation, whereas the latter relates to the non-phylogenetic part of the between-species variation.

The phylogenetic effects in both the *location* and *scale* parts are assumed to follow a multivariate normal distribution:

$$\begin{pmatrix} a_i^{(l)} \\ a_i^{(s)} \end{pmatrix} \sim \mathcal{N}\left(\begin{pmatrix} 0 \\ 0 \end{pmatrix}, \boldsymbol{\Sigma}_a \otimes \mathbf{A}\right), \tag{37}$$

$$\boldsymbol{\Sigma}_a = \begin{pmatrix} \sigma^2_{a(l)} & \rho_{a(ls)}\sigma_{a(l)}\sigma_{a(s)} \\ \rho_{a(ls)}\sigma_{a(l)}\sigma_{a(s)} & \sigma^2_{a(s)} \end{pmatrix}, \tag{38}$$

where $\sigma^2_{a(l)}$ and $\sigma^2_{a(s)}$ are the phylogenetic variances for the *location* and *scale* parts, respectively, and $\rho_{a(ls)}$ denotes the correlation between the phylogenetic effects in the two parts. The operator $\otimes$ denotes the Kronecker product, indicating that the covariance matrix is constructed by multiplying $\boldsymbol{\Sigma}_a$ with the phylogenetic correlation matrix $\mathbf{A}$ as defined earlier.

Similarly, the species-specific non-phylogenetic effects are modelled as:

$$\begin{pmatrix} e_i^{(l)} \\ e_i^{(s)} \end{pmatrix} \sim \mathcal{N}\left(\begin{pmatrix} 0 \\ 0 \end{pmatrix}, \boldsymbol{\Sigma}_e \otimes \mathbf{I}\right), \tag{39}$$

$$\boldsymbol{\Sigma}_e = \begin{pmatrix} \sigma^2_{e(l)} & \rho_{e(ls)}\sigma_{e(l)}\sigma_{e(s)} \\ \rho_{e(ls)}\sigma_{e(l)}\sigma_{e(s)} & \sigma^2_{e(s)} \end{pmatrix}, \tag{40}$$

where $\sigma^2_{e(l)}$ and $\sigma^2_{e(s)}$ are the non-phylogenetic species-level variances for the *location* and *scale* parts, respectively, and $\rho_{e(ls)}$ is the correlation between the non-phylogenetic effects in the two parts (cf. Nakagawa and Santos, 2012; Cinar et al., 2022). The interpretation of $\rho_{e(ls)}$ is similar to $\rho_{a(ls)}$ except that driving forces of such correlations are different; shared ancestry drives $\rho_{a(ls)}$ while shared environments drive $\rho_{e(ls)}$.

By including both phylogenetic and non-phylogenetic (random) effects at the species level, as well as individual-level residuals, this model allows us to partition the total phenotypic variance into components attributable to phylogeny, non-phylogenetic factors and within-species (individual) variation; phylogenetic effects are related to macro-evolutionary changes while non-phylogenetic effects micro-evolutionary changes (*sensu* Adams and Collyer, 2024). Such partitioning is particularly important and insightful when individual measurements are available, as it enables us to estimate the degree of trait convergence or divergence due to ecological and environmental factors beyond what is explained by shared ancestry.

Furthermore, the inclusion of random effects in both the *location* and *scale* parts, along with their potential correlations ($\rho_{a(ls)}$ and $\rho_{e(ls)}$), allows us to investigate whether species with higher mean trait values also exhibit higher variability, and whether these patterns are influenced by phylogenetic relationships or species-specific (non-phylogenetic) factors. It is interesting to note that in multivariate contexts, a positive non-phylogenetic correlation (ρ_e; e.g. $\rho_{e(l1l2)}$) can mean phenotypic integration not by genes but by environments (i.e., convergent evolution of trait means) while a positive $\rho_{e(s1s2)}$ could represent convergent evolution of trait variances (the model shown in the online tutorial).

In practical applications, this model can analyse data where multiple individuals are measured per species, such as morphological traits in animals or plants. By modelling both the mean and variance at multiple levels, we gain a more comprehensive understanding of the factors influencing trait evolution and variation within and among species. We note, however, that such datasets are still rare, and we will not provide an example of this model yet; we anticipate there are many opportunities for the application of individual-level PLSMs in the future.

3 Worked Examples

To illustrate the application of our phylogenetic location-scale models (PLSMs), we analyse a subset of the AVONET dataset (Tobias et al., 2022) focusing on 354 parrot species (Order: Psittaciformes), using avian phylogenetic trees from Jetz et al. (2012). This dataset, featuring traits such as body mass, beak size, and habitat, enables us to examine how mean trait values and variances evolve across species while incorporating phylogenetic relationships (Fig 5). The ecological and morphological diversity of Psittaciformes makes them an excellent group for demonstrating PLSMs' capacity to identify clade-specific variability and unravel evolutionary patterns of adaptation and diversification. As this is a methodological paper, the examples aim to showcase the potential of PLSMs rather than discover new patterns and deliver exhaustive biological interpretations. All implementations are performed using `brms` (v.2.22.0, Bürkner, 2017) in `R` (v.4.4.2), and all code and detailed output and descriptions are available at link), where we also show how to obtain phylogenetic heritability and macro-evolvability not shown in the examples below.

3.1 Different Trait Variance in Two Groups (Model 3)

We analysed beak length data from parrot species, contrasting forest-dwelling parrots with those inhabiting simpler, more open and less complex environments (e.g., grasslands, shrublands, and woodland). Using a phylogenetic location-scale model (i.e., Model 3, which is a simple version of Model 2), we estimated both the mean and variance parameters as functions of a categorical (binary) moderator that indicates whether parrots lived in forests or not (named `forest`). Let the response (y_i) be (log) centred beak length for species i ($\texttt{cbeak\_length}_i$), $\texttt{forest}_i \in \{0, 1\}$ the habitat indicator, and $\texttt{cmass}_i$ centred log body mass. The fitted PLSM (no phylogenetic random effect in the *scale* part) is:

$$\texttt{cbeak\_length}_i = \beta_0^{(l)} + \beta_{\texttt{cmass}}^{(l)}\,\texttt{cmass}_i + \beta_{\texttt{forest}}^{(l)}\,\texttt{forest}_i + a_i^{(l)} + e_i^{(l)}, \qquad \text{(location)}$$

$$\{a_i^{(l)}\} \sim \mathcal{N}\big(\mathbf{0},\, \sigma^2_{a(l)}\,\mathbf{A}\big)\,, \qquad \{e_i^{(l)}\} \sim \mathcal{N}\big(\mathbf{0},\, \sigma^2_{e_i(l)}\,\mathbf{I}\big)\,,$$

$$\ln\big(\sigma_{e_i(l)}\big) = \beta_0^{(s)} + \beta_{\texttt{cmass}}^{(s)}\,\texttt{cmass}_i + \beta_{\texttt{forest}}^{(s)}\,\texttt{forest}_i. \qquad \text{(scale)}$$

Here $\beta^{(l)}$ shift the clade-level mean (location), and $\beta^{(s)}$ reshape among-species dispersion (scale). A significant $\beta_{\texttt{forest}}^{(s)}$ implies heteroscedasticity between habitats.

The forest habitat did not significantly predict changes in the mean length of the beak ($\beta_{\texttt{forest}}^{(l)}$: 0.02, 95% CI: -0.01 to

0.05; note that we consider our results statistically significant when 95% CI is not spanning 0; Fig 5A & B), although beak length was tended to be larger for forest living parrots. In contrast, forest living did influence variances in beak length ($\beta^{(s)}_{\texttt{forest}}$: 0.96 (95% CI: 0.38 to 2.02); parrot species living in forests exhibit substantially greater variation in beak length than those in non-forest habitats (a $\tilde{1}60\%$ increase; $100[\exp(0.96) - 1] = 161.2$). Our model indicates that forest-dwelling parrot species exhibit higher evolutionary rates in beak shape than their non-forest counterparts. While this pattern is consistent with increased among-species variability, potentially reflecting greater evolvability in forest niches; it could also arise if forest environments are more heterogeneous, leading to faster shifts in adaptive optima. Additionally, greater phenotypic plasticity in response to variable resources or microhabitats could produce similar macro-evolutionary signatures. Disentangling these mechanisms would require complementary ecological or experimental data.

3.2 Co-evolution of Mean and Variance (Model 4)

In another application, we explored how mean trait values relate to their variance across species' geographical ranges, using Model 4. Let the response (y_i) be (log) centred geographical range size for species i ($\texttt{crange\_size}_i$) and $\texttt{cmass}_i$ centred log body mass. We modelled a phylogenetic effect in both parts with a correlation $\rho_{a(ls)}$:

$$\texttt{crange\_size}_i = \beta_0^{(l)} + \beta^{(l)}_{\texttt{cmass}}\,\texttt{cmass}_i + a_i^{(l)} + e_i^{(l)}, \qquad \text{(location)}$$

$$\ln\bigl(\sigma_{e_i(l)}\bigr) = \beta_0^{(s)} + \beta^{(s)}_{\texttt{cmass}}\,\texttt{cmass}_i + a_i^{(s)}, \qquad \text{(scale)}$$

$$\begin{pmatrix} a_i^{(l)} \\ a_i^{(s)} \end{pmatrix} \sim \mathcal{N}\left(\begin{pmatrix} 0 \\ 0 \end{pmatrix}, \boldsymbol{\Sigma}_a \otimes \mathbf{A}\right), \qquad \boldsymbol{\Sigma}_a = \begin{pmatrix} \sigma^2_{a(l)} & \rho_{a(ls)}\,\sigma_{a(l)}\sigma_{a(s)} \\ \rho_{a(ls)}\,\sigma_{a(l)}\sigma_{a(s)} & \sigma^2_{a(s)} \end{pmatrix},$$

$$e_i^{(l)} \sim \mathcal{N}\bigl(0,\, \sigma^2_{e_i(l)}\bigr).$$

A negative $\rho_{a(ls)}$ indicates that lineages with larger means exhibit reduced dispersion (a "ceiling/saturation" signature).

This phylogenetic location-scale model revealed a notable negative correlation between the intercepts of the *location* and *scale* parts at the phylogenetic level ($\rho_{a(ls)}$: -0.94, 95% CI: -1.00 to -0.82; Fig 5C, E, & G). The strong negative correlation at the phylogenetic level suggests that lineages with larger mean values are constrained in terms of how much additional variance they can accumulate. In other words, as mean values approach a "ceiling", the variance is homogenised. This pattern could suggest that parrot species with larger range sizes have similar ranges. In addition, range size variance increases significantly as body size increases (a $\tilde{2}0\%$ increase as 1 SD change in `cmass`; i.e., heteroscedasticity; $\beta^{(s)}_{\texttt{mass}}$: 0.18 (95% CI: 0.03 to 0.34; $100[\exp(0.18) - 1] = 19.72$).

3.3 Co-evolution of Two Traits (Model 5)

Finally, by using Model 5 (i.e., a bivariate phylogenetic location-scale model), we examined the co-evolution of two traits. Let the first response ($y_i^{(1)}$) be (log) centred beak width ($\texttt{cbreak\_width}_i$), the second response ($y_i^{(2)}$) , (log) centred beak depth ($\texttt{cbreak\_depth}_i$), and $\texttt{cmass}_i$ centred log body mass. We fitted a bivariate PLSM with phylogenetic random effects in both parts for both traits:

$$\begin{aligned} \texttt{cbreak\_width}_i &= \beta_0^{(l1)} + \beta^{(l1)}_{\texttt{cmass}}\,\texttt{cmass}_i + a_i^{(l1)} + e_i^{(l1)}, \\ \texttt{cbreak\_depth}_i &= \beta_0^{(l2)} + \beta^{(l2)}_{\texttt{cmass}}\,\texttt{cmass}_i + a_i^{(l2)} + e_i^{(l2)}, \end{aligned} \qquad \text{(location)}$$

$$\begin{aligned} \ln\bigl(\sigma_{e_{i(l1)}}\bigr) &= \beta_0^{(s1)} + \beta^{(s1)}_{\texttt{cmass}}\,\texttt{cmass}_i + a_i^{(s1)}, \\ \ln\bigl(\sigma_{e_{i(l2)}}\bigr) &= \beta_0^{(s2)} + \beta^{(s2)}_{\texttt{cmass}}\,\texttt{cmass}_i + a_i^{(s2)}. \end{aligned} \qquad \text{(scale)}$$

Stacking the four phylogenetic effects,

$$\begin{pmatrix} a_i^{(l1)} \\ a_i^{(l2)} \\ a_i^{(s1)} \\ a_i^{(s2)} \end{pmatrix} \sim \mathcal{N}\bigl(\mathbf{0},\ \boldsymbol{\Sigma}_a \otimes \mathbf{A}\bigr),$$

with

$$\boldsymbol{\Sigma}_a = \begin{pmatrix} \sigma^2_{a(l1)} & \rho_{a(l1l2)}\,\sigma_{a(l1)}\sigma_{a(l2)} & \rho_{a(l1s1)}\,\sigma_{a(l1)}\sigma_{a(s1)} & \rho_{a(l1s2)}\,\sigma_{a(l1)}\sigma_{a(s2)} \\ \cdot & \sigma^2_{a(l2)} & \rho_{a(l2s1)}\,\sigma_{a(l2)}\sigma_{a(s1)} & \rho_{a(l2s2)}\,\sigma_{a(l2)}\sigma_{a(s2)} \\ \cdot & \cdot & \sigma^2_{a(s1)} & \rho_{a(s1s2)}\,\sigma_{a(s1)}\sigma_{a(s2)} \\ \cdot & \cdot & \cdot & \sigma^2_{a(s2)} \end{pmatrix},$$

and residuals in the *location* parts

$$\begin{pmatrix} e_i^{(l1)} \\ e_i^{(l2)} \end{pmatrix} \sim \mathcal{N}\left(\begin{pmatrix} 0 \\ 0 \end{pmatrix}, \boldsymbol{\Sigma}_e \otimes \mathbf{I} \right), \quad \boldsymbol{\Sigma}_e = \begin{pmatrix} \sigma^2_{e(l1)} & \rho_{e(l1l2)}\,\sigma_{e(l1)}\sigma_{e(l2)} \\ \cdot & \sigma^2_{e(l2)} \end{pmatrix}.$$

Here $\rho_{a(l1l2)}$ (mean–mean), $\rho_{a(s1s2)}$ (variance–variance), and $\rho_{a(l1s2)}, \rho_{a(l2s1)}$ (cross mean–variance) are the four correlation types, summarised in Fig. 2.

We detected positive correlations not only between the means of these traits ($\rho_{a(l1l2)}$: 0.89, 95% CI: 0.82 to 0.94; Fig 5D, F, & H) but also between their variances (i.e., coevolution of the traits as well as co-divergence; $\rho_{a(s1s2)}$: 0.82, 95% CI: 0.48 to 0.98). Additionally, across-trait mean-variance correlations emerged; a positive correlation between the mean of beak width and the variance of beak depth was significant ($\rho_{a(l2s1)}$: 0.36, 95% CI: 0.02 to 0.65) while the other mean-variance correlation was positive albeit non-significant ($\rho_{a(l1s2)}$: 0.28, 95% CI: -0.04 to 0.56). The observed positive phylogenetic correlations between two traits are consistent with phenotypic (morphological) integration, a pattern of coordinated evolution among traits. Mechanistically, such integration can arise from shared genetic or developmental architecture (e.g., pleiotropy, modularity), correlated selection on functionally linked traits, or phenotypic plasticity along shared environmental gradients. Also, we repeat exercising caution when interpreting parameters involving phylogenetic variance on the *scale* part (i.e., $\rho_{a(s1s2)}, \rho_{a(l1s2)}, \rho_{a(l2s1)}$).

4 Discussion

We have introduced phylogenetic location-scale models (PLSMs) as a novel framework for jointly analysing the evolution of trait means and variances across species. By extending traditional phylogenetic comparative methods (specifically, PGLMM; Lynch, 1991; Hadfield and Nakagawa, 2010; Ives and Helmus, 2011) to model both the *location* and *scale* components of traits, we have provided a more comprehensive approach to understanding macroevolutionary patterns. Our approach models heteroscedasticity and allows for the investigation of coevolution between trait means and variances, both within and between traits.

One of the key insights from our work is the importance of considering trait variability alongside mean trait values in evolutionary studies. Traditional models that focus solely on mean traits may overlook significant evolutionary processes that influence trait dispersion across lineages. By modelling the variance explicitly, we can detect patterns such as increased variability associated with adaptive radiation or reduced variability due to stabilising selection. For example, in our application using the AVONET dataset (Tobias et al., 2022), we identified an ecological factor that explains heteroscedasticity in beak length (i.e., where variance in beak length was higher in forest living species).

Another key insight comes from our multivariate extension of PLSMs, which allows for exploring complex evolutionary relationships among multiple traits. By modelling the covariances between phylogenetic effects in both the *location* and *scale* parts, we can test hypotheses about evolutionary trade-offs, pleiotropy, and integration (Fig 3). This comprehensive modelling approach can reveal whether changes in one trait's mean or variance are associated with changes in another's, providing deeper insights into the mechanisms driving trait evolution.

More specifically, the ability to decompose the phylogenetic covariance structure into four distinct types of correlations is a significant advancement offered by our PLSM framework (Fig 3). These four correlations are: (1) *Across-trait mean-mean phylogenetic correlation* (coevolution), which examines how the evolutionary changes in the mean of one trait are associated with changes in the mean of another trait due to shared ancestry (Hansen and Martins, 1996; Cheverud, 1996); (2) *Across-trait variance-variance phylogenetic correlation* (co-divergence or contra-divergence), which explores whether the variability in one trait is evolutionarily linked to the variability in another trait, shedding light on coordinated evolution of trait variability (cf. Hansen and Houle, 2008); (3) *Within-trait mean-variance phylogenetic correlation*, which assesses whether species with higher (or lower) mean trait values also tend to have higher (or lower) variability in the same trait, indicating potential evolutionary constraints or diversification (cf. Revell et al., 2008); and (4) *Across-trait mean-variance phylogenetic correlation*, which investigates whether the mean of one trait is evolutionarily associated with the variance of another trait, suggesting complex evolutionary interactions such as a shift in one trait relaxing selection on another (Fig 2). By explicitly modelling these correlations, we can disentangle the multifaceted relationships among traits and their variances, providing a nuanced understanding of evolutionary processes.

Of relevance, several earlier and existing phylogenetic comparative methods (PCMs) speak to heterogeneity and heteroscedasticity. First, "regime-based" models compare evolutionary rate–covariance matrices across clades or discrete regimes mapped onto the tree, testing whether evolutionary covariances differ among lineages classified by a categorical character (e.g., Revell and Collar, 2009; Caetano and Harmon, 2017; Hermansen et al., 2018). These methods are powerful for asking whether the mean-process (e.g., Brownian motion rate matrices) changes by regime, but they typically treat residual dispersion as a nuisance term rather than a modelling target. Second, the Fabric model and its recent multi-variable extension identify branches where evolutionary rates and covariances shift by transforming branch lengths, allowing among-clade differences in variability/evolvability to be detected without *a priori* regime assignments (Pagel et al., 2022; Pagel and Meade, 2025). In contrast, PLSMs treat the log residual standard deviation as an explicit, evolvable response with its own fixed and phylogenetic effects, estimated jointly with the mean. This distributional, multi-response formulation yields quantities that are difficult to obtain in the alternatives, most notably the four classes of phylogenetic correlations (mean–mean, variance–variance, within-trait mean–variance, and across-trait mean–variance), as well as $H^2_{(s)}$ and $CV_{A(s)}$. Thus, PLSMs complement regime-based and branch-shift approaches by modelling how dispersion evolves and how it covaries with means, rather than only where rate structure changes on the tree. In other words, with PLSMs, the evolution of variation becomes a central target of research (cf. Rohlfs et al., 2014; Silvestro et al., 2015; Gaboriau et al., 2020).

As summarised in Figure 3, we can convert these four correlation classes, which only PLSMs could directly obtain, as far as we are aware, into concrete examples of macro-evolutionary patterns. First, anatomical integration or pleiotropy, shared genetic or developmental pathways, should yield positive mean-mean and variance-variance correlations, because the same loci drive coordinated shifts in both the averages and the lability of multiple traits (Wagner and Altenberg, 1996; Pigliucci, 2003). Second, life-history trade-offs impose allocation limits that favour inverse relationships between competing functions; this generates negative mean-mean correlations (e.g. clutch size vs. egg size) (Stearns, 1992). Yet, whether life-history also induces correlations involving variance is an open question. Third, during adaptive radiation, an ecological opportunity relaxes constraints across or selects many trait axes simultaneously. Although correlated evolution of means is unpredictable, adaptive radiation should generate positive variance-variance correlation, a pattern we term "co-divergence" (Schluter, 2000). Fourth, saturation or ceiling effects arise when a trait approaches a physiological or environmental limit (e.g., maximum dispersal range); the mean plateaus while among-lineage variance is squeezed, leaving a distinctive negative mean-variance signature (cf. Brown, 1995). Finally, "contra-divergence" describes the reciprocal case in which directional change in one trait constrains the evolutionary lability of another, producing negative variance-variance correlations. For example, increasing complexity in bird song is accompanied by reduced variability in plumage signals (cf. Badyaev et al., 2002; Cooney et al., 2018). Although not an exhaustive list of potential macro-evolutionary relationships, the examples are readily testable with existing comparative data.

In conclusion, PLSMs offer a powerful and flexible framework for exploring the evolution of trait means and variances. By leveraging extensive trait data such as AVONET and FishBase (Froese and Pauly, 2000) and comprehensive phylogenies, researchers can uncover broad patterns and test overarching hypotheses about trait evolution. By accounting for both aspects of trait distribution, researchers can gain a more nuanced understanding of evolutionary dynamics. We encourage the adoption of PLSMs in comparative studies and suggest that they have the potential to reveal novel insights into the mechanisms driving trait evolution. Although more future developments are necessary (see **Box 1**), applying PLSMs will likely become much more accessible as computational tools and resources advance. Importantly, PLSMs allow us to reanalyse almost all comparative datasets published previously, offering fresh insights and potentially revising earlier conclusions (Nakagawa et al., 2025a). Such future work may lead to a deeper understanding of how evolutionary processes shape biodiversity and how traits influence the ecological roles of species.

Table 1: Key notations for phylogenetic location–scale models, PLSMs (see the main text for mathematical definitions and extended explanations).

Notation	**Definition (biological meaning)**
y_i	Observed trait value for species i (typically a species mean on the analysis scale). Realised phenotype at the tips. Also, $\mathbf{y}_i = (y_i^{(1)}, y_i^{(2)}, \ldots)$ is a vector of multiple traits for species i in multivariate PLSMs; used to study phenotypic integration, trade-offs, and modularity.
y_{ij}	Observation j from species i (individual-level data). Separates within-species variation from among-species patterns.
x_{ki}, x_{kij}	Predictor k for species i (or individual j in species i). Ecology, environment, or life history that may shift means or dispersion.
$\beta_0^{(l)}$, $\beta_k^{(l)}$	Intercept and slopes in the *location* (mean) model; quantify how predictors shift clade-level averages.
$\beta_0^{(s)}$, $\beta_k^{(s)}$	Intercept and slopes in the *scale* model for $\ln(\sigma_{e_i(l)})$; quantify how predictors reshape among-species dispersion (heteroscedasticity).
$a_i^{(l)}$	Phylogenetic random effect (location): lineage-level deviation in mean due to shared ancestry (macro-evolutionary signal in trait averages).
$a_i^{(s)}$	Phylogenetic random effect (scale): lineage-level deviation in log residual SD; captures clade-specific lability/canalisation (variance evolution).
$e_i^{(l)}$	Species-level non-phylogenetic random effect in the *location* part; among-species variation not explained by shared ancestry (e.g., convergent environments).
$\varepsilon_{ij}^{(l)}$	Individual-level residual (within-species variation). Distinct from $e_i^{(l)}$, which is among-species.
$\sigma^2_{a(l)}$	Phylogenetic variance of $a^{(l)}$; magnitude of among-lineage divergence in trait means.
$\sigma^2_{a(s)}$	Phylogenetic variance of $a^{(s)}$; magnitude of among-lineage divergence in dispersion (how strongly heteroscedasticity is phylogenetically structured).
$\rho_{a(ls)}$	Phylogenetic correlation between $a^{(l)}$ and $a^{(s)}$ (within-trait mean–variance coevolution). $\rho_{a(ls)} < 0$ suggests ceilings/saturation; $\rho_{a(ls)} > 0$ suggests co-divergence.
$\mathbf{A}$	Phylogenetic correlation matrix from a ultrametric tree; encodes shared evolutionary time and structures all phylogenetic effects
$\ln(\sigma_{e_i(l)})$	Species-specific residual SD on the natural logarithm scale (ln), the response in the *scale* part; treats dispersion as an evolvable/conditioned trait.
$\overline{\sigma^2}_{e(l)}$	Average residual variance in the *location* part (on the data scale); background scatter after accounting for phylogeny and fixed effects on the mean part.
$\mathbf{\Sigma}_a$	Variance–covariance (VCV) matrix of phylogenetic effects across parts/traits; with $\mathbf{A}$ gives $\mathbf{\Sigma}_a \otimes \mathbf{A}$, encoding coevolution in mean and variance.
$\mathbf{\Sigma}_e$	VCV of residuals among traits in the *location* part; allows residual mean–mean coupling beyond phylogeny (environmental/convergent effects).
$\rho_{a(l_1 l_2)}$	Across-trait phylogenetic correlation of means (coevolution via pleiotropy/integration vs. trade-offs).
$\rho_{a(s_1 s_2)}$	Across-trait phylogenetic correlation of variances ("co-divergence" or "contra-divergence" of lability).
$\rho_{a(l_1 s_1)}$, $\rho_{a(l_2 s_2)}$	Within-trait phylogenetic mean–variance correlations (do lineages with larger means show greater or lower dispersion in the same trait?).
$\rho_{a(l_1 s_2)}$, $\rho_{a(l_2 s_1)}$	Across-trait phylogenetic mean–variance correlations (e.g., shift in trait 1 relaxes or constrains variability in trait 2).
$H^2_{(l)}$, $H^2_{(s)}$	Phylogenetic heritability (*location* and *scale*): Fractions of variance attributable to shared ancestry in trait means (l) and variances (s).
$CV_{A(l)}$, $CV_{A(s)}$	Macro-evolvability (*location* and *scale*): Mean-standardised potential for evolutionary change in trait means (l) and variances (s).
$\sigma^2_{f(l)}$, $\sigma^2_{f(s)}$	Variance due to fixed effects in location/scale: $\mathrm{Var}\big(\sum_k \beta_k^{(l)} x_{ki}\big)$ and $\mathrm{Var}\big(\sum_k \beta_k^{(s)} x_{ki}\big)$; deterministic components (ecology, environment).
σ^2_p	Phenotypic variance for the *location* part on the data scale; basis for $H^2_{(l)}$ (sum of fixed, phylogenetic, and residual components).

Box 1: Limitations and future opportunities in PLSMs

We have some potential limitations in PLSMs to address, especially in future work. Most notably, the increased complexity of these models requires careful statistical handling. Estimating covariance structures, especially in multivariate models, can be computationally demanding and may require larger datasets for reliable parameter estimates (cf. Cinar et al., 2022). Although advanced statistical software and computational techniques, such as Bayesian methods implemented in `brms` (as in our example) or direct use of `Stan` (Carpenter et al., 2017), can facilitate the fitting of these complex models, PLSMs with large datasets may take prohibitively long computational times. Optimising code efficiency and leveraging high-performance computing resources could mitigate some of these challenges (e.g, our most complex model, i.e., bivariate PLSM, took approximately 122 hours to run on a Mac computer: Apple M1 Ultra with 128 GB memory).

Another consideration is the interpretation of the correlations between phylogenetic effects. While significant correlations provide evidence for coevolutionary patterns, distinguishing between causation and correlation remains challenging. Integrating these findings with biological knowledge about the traits and species under study is essential to drawing meaningful conclusions about the underlying evolutionary mechanisms. Of relevance, integrating PLSMs with causal modelling frameworks (McElreath, 2018), such as phylogenetic path analysis or structural equation modelling, could provide a more holistic view of the evolutionary relationships among traits (Hardenberg and Gonzalez-Voyer, 2013).

Additionally, future research can extend the PLSM framework in several ways. One promising direction is to apply PLSMs to non-Gaussian traits (Nakagawa et al., 2025b), such as count data (e.g., using negative binomial models for overdispersed Poisson data; Ver Hoef and Boveng, 2007), proportion data (e.g., using beta regression models; Douma and Weedon, 2019; Burke et al., 2023; Korhonen et al., 2024), or ordinal data (e.g., threshold models; Martin et al., 2017). Such an extension would broaden the applicability of PLSMs to a wider range of traits and datasets commonly encountered in evolutionary biology. Also, incorporating measurement error and accounting for uncertainty in phylogenetic relationships could enhance the robustness of the models (Cornwell and Nakagawa, 2017; Nakagawa and De Villemereuil, 2019). Methods to integrate phylogenetic uncertainty, such as Bayesian approaches that sample from posterior distributions of phylogenies, would provide more accurate estimates of evolutionary parameters with more appropriate degrees of uncertainty. Further, here we only considered the Brownian motion model of evolution, yet other models, such as the Ornstein–Uhlenbeck process, can be tested by using different specifications of phylogenetic correlation matrix and checking model fit (e.g., likelihood ratio tests) (Cornwell and Nakagawa, 2017; Pottier et al., 2024).

It should also be noted that a different way of fitting the *scale* part; indeed, the alternative way has as many *scale* parts as the number of random factors (including residuals). For example, using Equations 7-8 (i.e. Model 2), we can have a location-scale model as follows (note we have numbered hyper-scripts to distinguish from other location-scale models in the main text):

$$y_i = \beta_0^{(l1)} + \sum_{k=1}^{K} \beta_k^{(l1)} x_{ki} + a_i^{(l1)} + e_i^{(l1)}, \tag{41}$$

$$\ln(\sigma_{a_i}) = \beta_0^{(s1)} + \sum_{k=1}^{K} \beta_k^{(s1)} x_{ki}, \tag{42}$$

and

$$\ln(\sigma_{e_i}) = \beta_0^{(s2)} + \sum_{k=1}^{K} \beta_k^{(s2)} x_{ki}. \tag{43}$$

As one can see, it has two *scale* parts, although the *scale* parts cannot have random effects in this formulation. Whether such formulations are useful depends on questions in hand (cf. Williams et al., 2021; Rodriguez et al., 2023; King et al., 2025). Interestingly, this formulation is probably more comparable to the Fabric model (Pagel et al., 2022; Pagel and Meade, 2025), because it models phylogenetic standard deviation directly as well as residual standard deviation; the Fabric model also directly works with phylogenetic variance (standard deviation). One disadvantage of the above formulation is that currently, we cannot implement this model using `brms`.

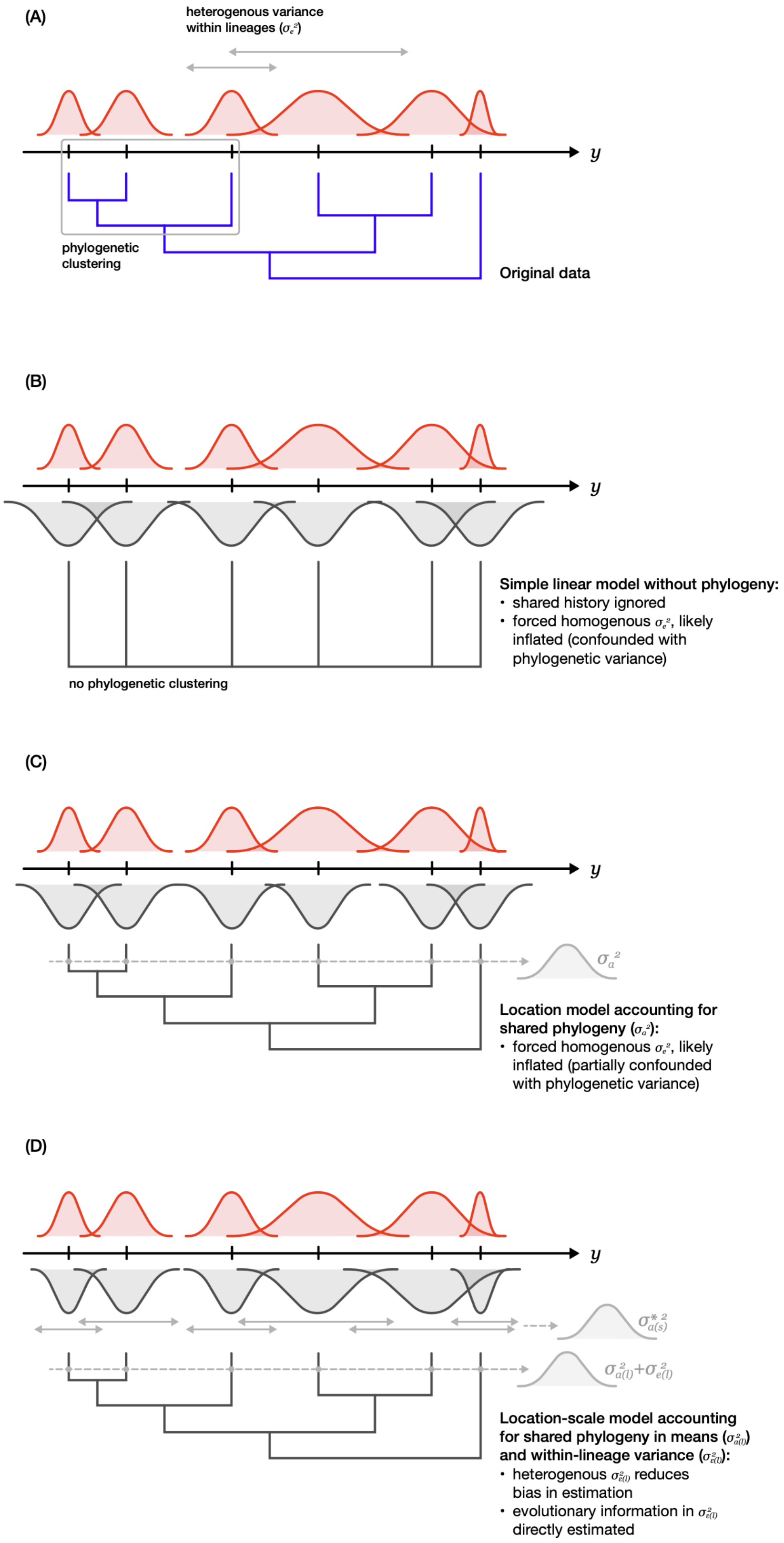

Figure 1: Concept: evolution of mean and variance

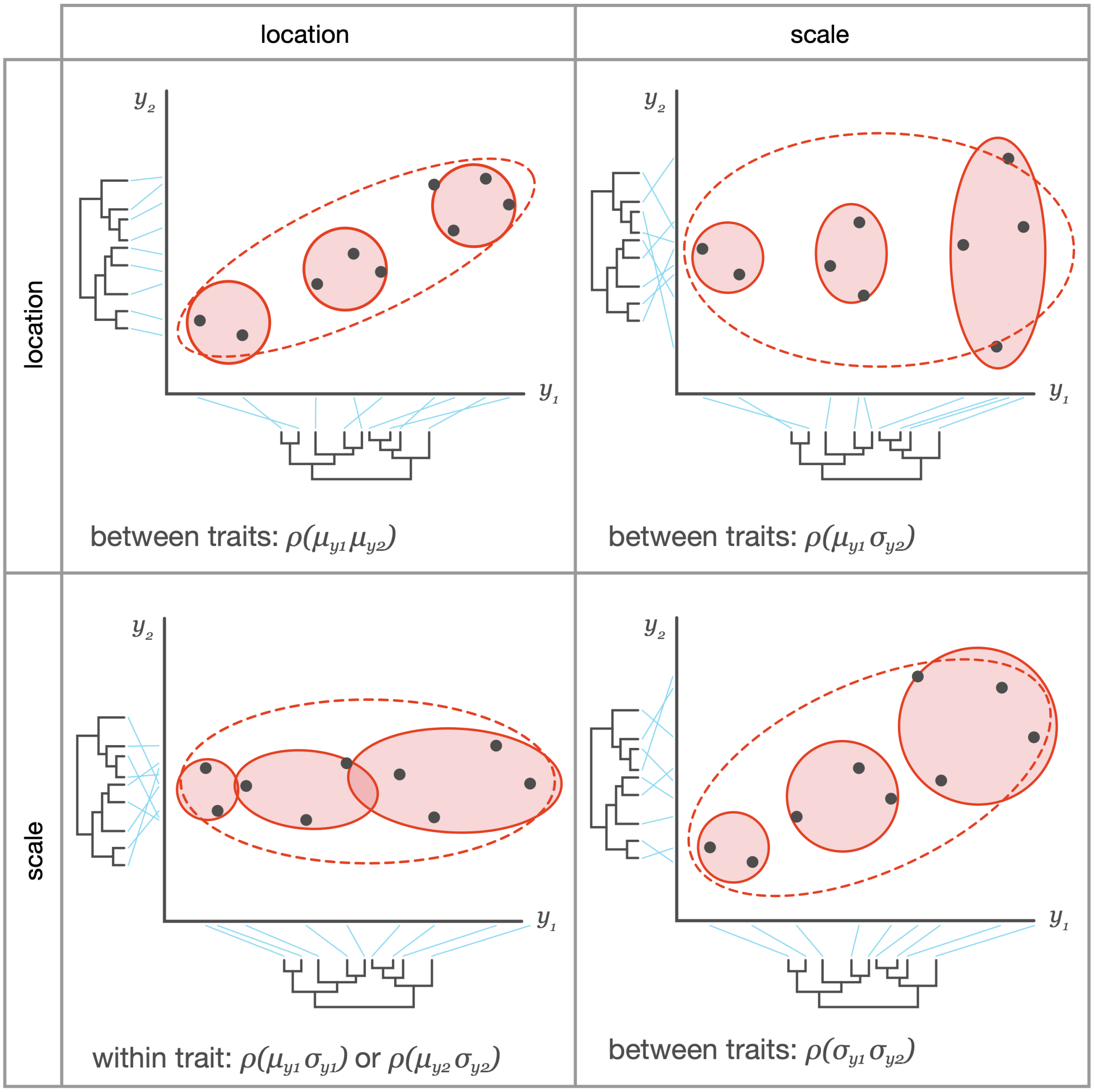

Figure 2: Matrix of co-evolution

mechanism	location-scale VCV pattern	biological examples
anatomic integration pleiotropy	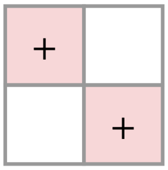	bird beak* 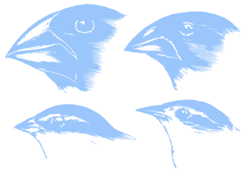
life history trade-offs	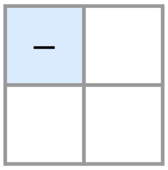	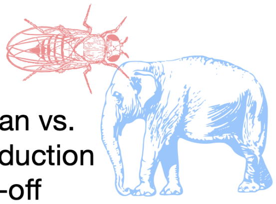 lifespan vs. reproduction trade-off
codivergence adaptive radiation	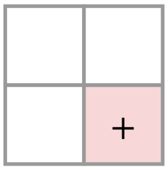	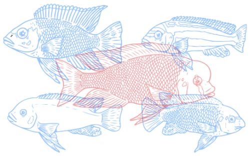 cichlids radiation
saturation ceiling effect	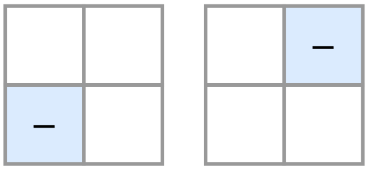	variation in bird range sizes* 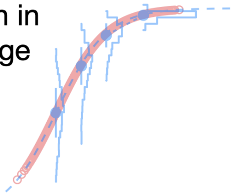
contradivergence	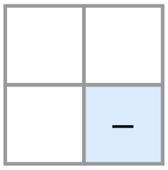	coevolution of bird song vs. ornament variability 

*See also the provided numerical examples

Possible predicted correlations:

	loc	scale
loc	B	B
scale	W	B

Matrix layout as in Fig. X: correlations are considered between (B) or within (W) traits.

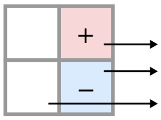

positive correlation
negative correlation
no clear prediction

Figure 3: Biological mechanisms

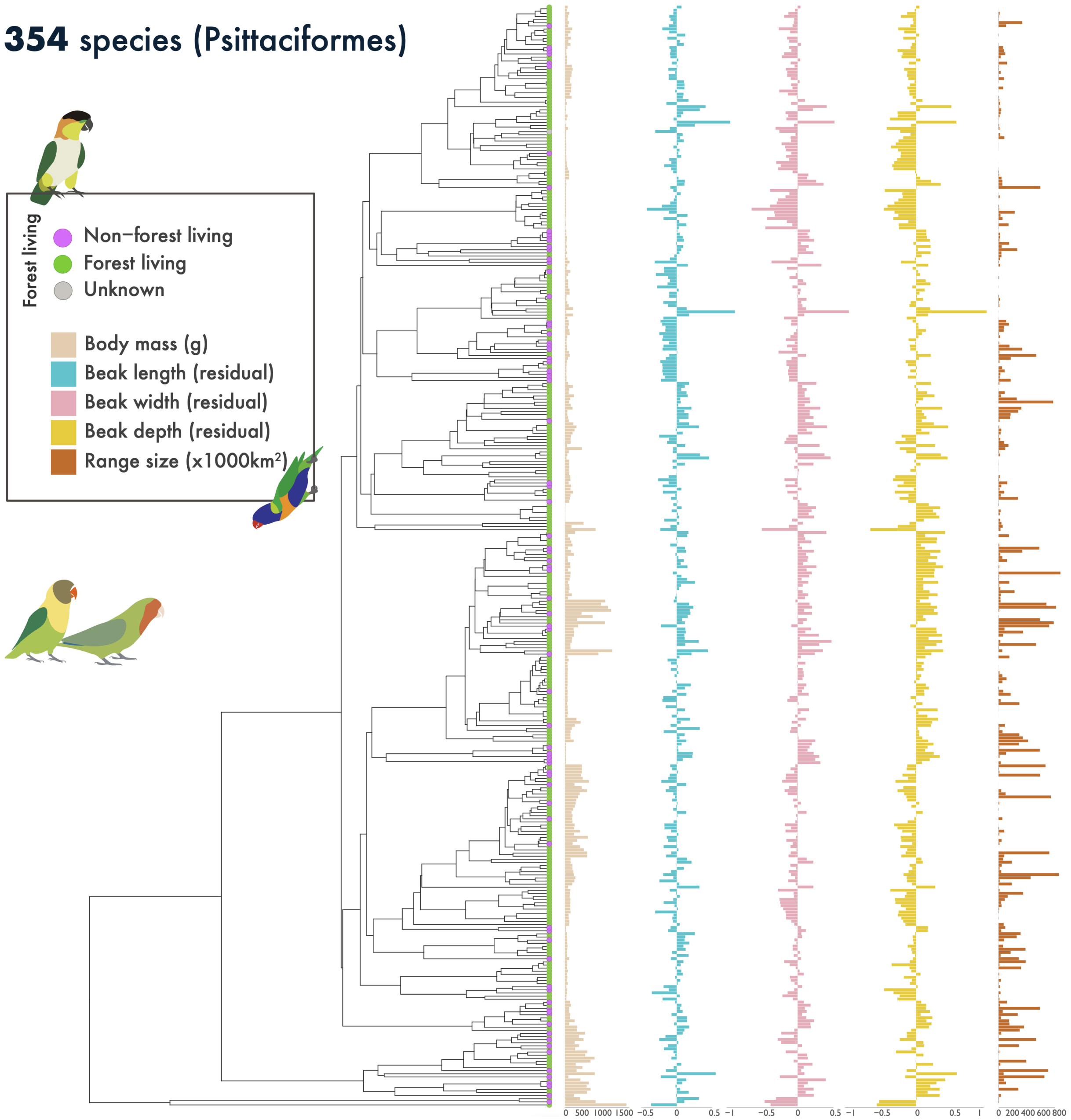

Figure 4: Parrot data visualization

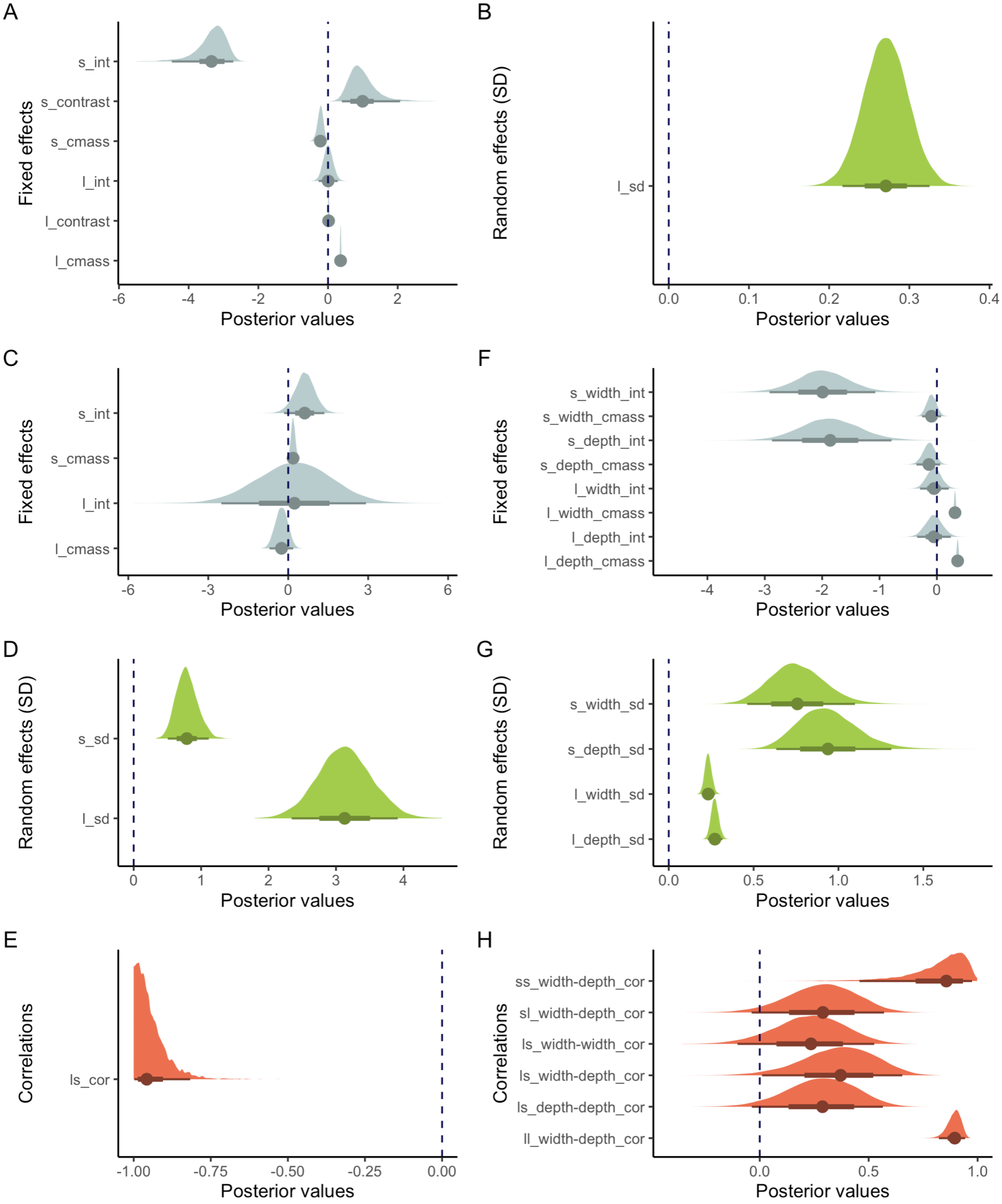

Figure 5: Results of our 3 examples

5 Figure legends

FIGURE 1 Conceptual illustration of phylogenetic location-scale models (PLSMs). (A) Hypothetical trait data illustrating both differences in trait means and heterogeneous variance among species or clades (heteroscedasticity). Traditional analyses often ignore phylogeny and heteroscedasticity, potentially overlooking crucial macroevolutionary patterns. (B) A conventional regression model ignoring phylogenetic relationships assumes equal variance across species, neglecting heterogeneity due to shared ancestry. (C) A phylogenetic (location) model incorporates phylogenetic relationships (depicted by the tree below), addressing correlations in trait means arising from shared evolutionary history yet still assuming homogeneous variance across species. (D) The phylogenetic location-scale model (PLSM), proposed here, extends further by simultaneously modelling both trait means (*location*) and variances (*scale*). This model accounts for heteroscedasticity and allows variance to vary among clades, explicitly separating variance due to phylogeny.

FIGURE 2 Illustration of the four types of phylogenetic correlations (variance-covariance, VCV), captured by the phylogenetic location-scale model (PLSM). Each panel depicts hypothetical scenarios for two traits (y_1, y_2) across species, highlighting different forms of correlated evolution in trait means (*location*) and variances (*scale*). The top-left panel (location–location correlation) represents correlations between trait means ($\rho(\mu_{y_1}, \mu_{y_2})$), showing how evolutionary shifts in the mean of one trait are associated with shifts in the mean of another due to shared ancestry. The top-right panel (location–scale) illustrates the relationship between the mean of one trait (μ_{y_1}) and the variance of another (σ_{y_2}), indicating whether evolutionary changes in the mean of one trait coincide with changes in variability of another. The bottom-left panel (within-trait location–scale) illustrates the correlation between the mean and variance of the same trait (μ_{y_1}, σ_{y_1}) or (μ_{y_2}, σ_{y_2}), indicating potential evolutionary constraints or diversification within traits. Finally, the bottom-right panel (scale–scale) demonstrates correlations between variances of two different traits (σ_{y_1}, σ_{y_2}), indicating coordinated evolutionary changes in trait variability. Ellipses represent phylogenetic patterns, with each ellipsis indicating trait distributions of species within a clade.

FIGURE 3 Examples of how evolutionary mechanisms may be detected through distinct patterns in location-scale variance-covariance (VCV) structures, accompanied by biological examples. The left column lists evolutionary mechanisms (anatomic integration/pleiotropy, life-history trade-offs, adaptive radiation, and saturation/ceiling effects). The central column visualises the expected phylogenetic correlation patterns between trait means (*location*) and variances (*scale*), where "+" indicates a positive correlation, and "−" indicates a negative correlation. The right column provides biological scenarios exemplifying each mechanism, including morphological integration in bird beaks, life-history trade-offs in reproductive traits, trait diversification during cichlid adaptive radiations, and constraints on variability such as range-size saturation in birds. The bottom inset clarifies how correlations are interpreted within or between traits, with colours indicating predicted positive (red) or negative (blue) correlations and blank spaces representing cases where no precise directional prediction can be made. Note that these mechanisms are not exhaustive but rather illustrative.

FIGURE 4 Trait distributions and ecological characteristics of 354 parrot species (Order: Psittaciformes) from the AVONET dataset (Tobias et al., 2022). Panels show residual morphological traits (beak length, width, depth) and body mass, categorised by forest-living (green) and non-forest-living species (purple), along with their geographical range size (in thousands of km^2). Trait residuals were calculated after correcting for body size. This dataset, combined with a tree from Jetz et al. (2012) phylogenetic tree, serves as our illustrative example for applying phylogenetic location-scale models (PLSMs).

FIGURE 5 Posterior distributions of parameters from three worked examples of phylogenetic location-scale models (PLSMs), fitted to parrot morphological traits. Panels (A & B) show results from the example for Model 3, examining the effect of habitat (forest vs. non-forest) on mean (location: `l`) and variance (scale; indicated by `s`) of beak length (`int`: intercept; `contrast`: forest vs non-forest; `cmass`: body mass centred on log scale). Panels (C, D, & E) illustrate the example for Model 4, which models the size of the geographical range with fixed effects for mean (location, `l`) and variance (scale, `s`), two types of phylogenetic standard deviations (`s_sd` and `l_sd`), and the correlation (`ls_cor`) between phylogenetic effects of *location* and *scale* components, indicating the coevolution mean-variance. Panels (F, G, & H) display the example for Model 5, a bivariate analysis of beak width and depth, showing fixed effects intercept (`int`) and centered body mass (`cmass`) for both traits' *location* and *scale* parts of the traits, their phylogenetic standard deviations, and correlations (`ll`: mean–mean; `ss`: variance–variance; `ls` and `sl`: mean–variance). The vertical dashed lines indicate zero; points show posterior medians, thick intervals denote 66% credible intervals, and thin whiskers represent 95% credible intervals.

References

D. C. Adams and M. L. Collyer. Extending phylogenetic regression models for comparing within-species patterns across the tree of life. *Methods in Ecology and Evolution*, 15(12):2234–2246, 2024.

A. V. Badyaev, G. E. Hill, and B. V. Weckworth. Species divergence in sexually selected traits: increase in song elaboration is related to decrease in plumage ornamentation in finches. *Evolution*, 56(2):412–419, 2002.

J. H. Brown. *Macroecology*. University of Chicago Press, Chicago, IL, 1995.

M. Bruijning, C. J. E. Metcalf, E. Jongejans, and J. F. Ayroles. The evolution of variance control. *Trends in ecology & evolution*, 35(1):22–33, 2020.

S. Burke, P. Pottier, M. Lagisz, E. L. Macartney, T. Ainsworth, S. M. Drobniak, and S. Nakagawa. The impact of rising temperatures on the prevalence of coral diseases and its predictability: A global meta-analysis. *Ecology letters*, 26(8):1466–1481, 2023.

P.-C. Bürkner. brms: An r package for bayesian multilevel models using stan. *Journal of statistical software*, 80:1–28, 2017.

D. S. Caetano and L. J. Harmon. ratematrix: an r package for studying evolutionary integration among several traits on phylogenetic trees. *Methods in Ecology and Evolution*, 8(12):1920–1927, 2017.

B. Carpenter, A. Gelman, M. D. Hoffman, D. Lee, B. Goodrich, M. Betancourt, M. A. Brubaker, J. Guo, P. Li, and A. Riddell. Stan: A probabilistic programming language. *Journal of statistical software*, 76, 2017.

J. M. Cheverud. Developmental integration and the evolution of pleiotropy. *American Zoologist*, 36(1):44–50, 1996.

O. Cinar, S. Nakagawa, and W. Viechtbauer. Phylogenetic multilevel meta-analysis: A simulation study on the importance of modelling the phylogeny. *Methods in Ecology and Evolution*, 13(2):383–395, 2022.

I. R. Cleasby and S. Nakagawa. Neglected biological patterns in the residuals: a behavioural ecologist's guide to co-operating with heteroscedasticity. *Behavioral Ecology and Sociobiology*, 65:2361–2372, 2011.

I. R. Cleasby, S. Nakagawa, and H. Schielzeth. Quantifying the predictability of behaviour: statistical approaches for the study of between-individual variation in the within-individual variance. *Methods in Ecology and Evolution*, 6 (1):27–37, 2015.

C. R. Cooney, H. E. MacGregor, N. Seddon, and J. A. Tobias. Multi-modal signal evolution in birds: re-examining a standard proxy for sexual selection. *Proceedings of the Royal Society B*, 285(1889):20181557, 2018.

C. K. Cornwallis and A. S. Griffin. A guided tour of phylogenetic comparative methods for studying trait evolution. *Annual Review of Ecology, Evolution, and Systematics*, 55, 2024.

W. Cornwell and S. Nakagawa. Phylogenetic comparative methods. *Current Biology*, 27(9):R333–R336, 2017.

J. C. Douma and J. T. Weedon. Analysing continuous proportions in ecology and evolution: A practical introduction to beta and dirichlet regression. *Methods in Ecology and Evolution*, 10(9):1412–1430, 2019.

J. Felsenstein. Phylogenies and the comparative method. *The American Naturalist*, 125(1):1–15, 1985.

R. Froese and D. Pauly. *FishBase 2000: concepts designs and data sources*, volume 1594. WorldFish, 2000.

T. Gaboriau, F. K. Mendes, S. Joly, D. Silvestro, and N. Salamin. A multi-platform package for the analysis of intra-and interspecific trait evolution. *Methods in Ecology and Evolution*, 11(11):1439–1447, 2020.

T. Garland, Jr and A. R. Ives. Using the past to predict the present: confidence intervals for regression equations in phylogenetic comparative methods. *The American Naturalist*, 155(3):346–364, 2000.

A. Haber. Phenotypic covariation and morphological diversification in the ruminant skull. *The American Naturalist*, 187(5):576–591, 2016.

J. Hadfield and S. Nakagawa. General quantitative genetic methods for comparative biology: phylogenies, taxonomies and multi-trait models for continuous and categorical characters. *Journal of evolutionary biology*, 23(3):494–508, 2010.

B. Halliwell. Rethinking niche conservatism with phylogenetic location-scale models. *bioRxiv*, pages 2025–03, 2025.

T. F. Hansen and D. Houle. Measuring and comparing evolvability and constraint in multivariate characters. *Journal of evolutionary biology*, 21(5):1201–1219, 2008.

T. F. Hansen and E. P. Martins. Translating between microevolutionary process and macroevolutionary patterns: the correlation structure of interspecific data. *Evolution*, 50(4):1404–1417, 1996.

T. F. Hansen, J. Pienaar, and S. H. Orzack. A comparative method for studying adaptation to a randomly evolving environment. *Evolution*, 62(8):1965–1977, 2008.

A. v. Hardenberg and A. Gonzalez-Voyer. Disentangling evolutionary cause-effect relationships with phylogenetic confirmatory path analysis. *Evolution*, 67(2):378–387, 2013.

J. S. Hermansen, J. Starrfelt, K. L. Voje, and N. C. Stenseth. Macroevolutionary consequences of sexual conflict. *Biology Letters*, 14(6):20180186, 2018.

W. G. Hill and H. A. Mulder. Genetic analysis of environmental variation. *Genetics research*, 92(5-6):381–395, 2010.

D. Houle. Comparing evolvability and variability of quantitative traits. *Genetics*, 130(1):195–204, 1992.

E. A. Housworth, E. P. Martins, and M. Lynch. The phylogenetic mixed model. *The American Naturalist*, 163(1): 84–96, 2004.

G. Hunt. The relative importance of directional change, random walks, and stasis in the evolution of fossil lineages. *Proceedings of the National Academy of Sciences*, 104(47):18404–18408, 2007.

A. R. Ives and M. R. Helmus. Generalized linear mixed models for phylogenetic analyses of community structure. *Ecological Monographs*, 81(3):511–525, 2011.

W. Jetz, G. H. Thomas, J. B. Joy, K. Hartmann, and A. O. Mooers. The global diversity of birds in space and time. *Nature*, 491(7424):444–448, 2012.

J. G. King, J. L. Pick, and J. D. Hadfield. Quantifying the correlation between variance components: an extension to the double-hierarchical generalised linear model. *EcoEvoRxiv*, 2025.

P. Korhonen, F. K. Hui, J. Niku, S. Taskinen, and B. van der Veen. A comparison of joint species distribution models for percent cover data. *Methods in Ecology and Evolution*, 15(12):2359–2372, 2024.

Y. Lee and J. A. Nelder. Hierarchical generalized linear models. *Journal of the Royal Statistical Society Series B: Statistical Methodology*, 58(4):619–656, 1996.

Y. Lee and J. A. Nelder. Double hierarchical generalized linear models (with discussion). *Journal of the Royal Statistical Society Series C: Applied Statistics*, 55(2):139–185, 2006.

M. Lynch. The rate of morphological evolution in mammals from the standpoint of the neutral expectation. *The American Naturalist*, 136(6):727–741, 1990.

M. Lynch. Methods for the analysis of comparative data in evolutionary biology. *Evolution*, 45(5):1065–1080, 1991.

G. Marroig, L. T. Shirai, A. Porto, F. B. de Oliveira, and V. De Conto. The evolution of modularity in the mammalian skull ii: evolutionary consequences. *Evolutionary Biology*, 36(1):136–148, 2009.

J. G. Martin, E. Pirotta, M. B. Petelle, and D. T. Blumstein. Genetic basis of between-individual and within-individual variance of docility. *Journal of Evolutionary Biology*, 30(4):796–805, 2017.

R. McElreath. *Statistical rethinking: A Bayesian course with examples in R and Stan.* Chapman and Hall/CRC, 2018.

H. A. Mulder, P. Bijma, and W. G. Hill. Selection for uniformity in livestock by exploiting genetic heterogeneity of residual variance. *Genetics Selection Evolution*, 40:1–23, 2008.

H. A. Mulder, P. Gienapp, and M. E. Visser. Genetic variation in variability: Phenotypic variability of fledging weight and its evolution in a songbird population. *Evolution*, 70(9):2004–2016, 2016.

S. Nakagawa and P. De Villemereuil. A general method for simultaneously accounting for phylogenetic and species sampling uncertainty via rubin's rules in comparative analysis. *Systematic Biology*, 68(4):632–641, 2019.

S. Nakagawa and E. S. Santos. Methodological issues and advances in biological meta-analysis. *Evolutionary Ecology*, 26:1253–1274, 2012.

S. Nakagawa and H. Schielzeth. A general and simple method for obtaining r2 from generalized linear mixed-effects models. *Methods in ecology and evolution*, 4(2):133–142, 2013.

S. Nakagawa, A. Mizuno, K. Morrison, L. Ricolfi, C. Williams, S. M. Drobniak, M. Lagisz, and Y. Yang. Location-scale meta-analysis and meta-regression as a tool to capture large-scale changes in biological and methodological heterogeneity: A spotlight on heteroscedasticity. *Global Change Biology*, 31(5):e70204, 2025a.

S. Nakagawa, S. Ortega, E. Gazzea, M. Lagisz, A. Lenz, E. Lundgren, and A. Mizuno. Location–scale models in ecology and evolution: heteroscedasticity in continuous, count and proportion data. *EcoEvoRxiv*, 2025b. doi: https://doi.org/10.32942/X2WH17.

R. E. O'Dea, D. W. Noble, and S. Nakagawa. Unifying individual differences in personality, predictability and plasticity: a practical guide. *Methods in Ecology and Evolution*, 13(2):278–293, 2022.

M. Pagel. Inferring the historical patterns of biological evolution. *Nature*, 401(6756):877–884, 1999.

M. Pagel and A. Meade. Trait macroevolution in the presence of covariates. *Nature Communications*, 16(1):4555, 2025.

M. Pagel, C. O'Donovan, and A. Meade. General statistical model shows that macroevolutionary patterns and processes are consistent with darwinian gradualism. *Nature communications*, 13(1):1113, 2022.

W. D. Pearse, T. J. Davies, and E. Wolkovich. How to define, use, and interpret pagel's λ λ (lambda) in ecology and evolution. *Global Ecology and Biogeography*, 34(4):e70012, 2025.

M. Pigliucci. Phenotypic integration: studying the ecology and evolution of complex phenotypes. *Ecology letters*, 6 (3):265–272, 2003.

A. Porto, F. B. de Oliveira, L. T. Shirai, V. De Conto, and G. Marroig. The evolution of modularity in the mammalian skull i: morphological integration patterns and magnitudes. *Evolutionary Biology*, 36(1):118–135, 2009.

P. Pottier, D. W. Noble, F. Seebacher, N. C. Wu, S. Burke, M. Lagisz, L. E. Schwanz, S. M. Drobniak, and S. Nakagawa. New horizons for comparative studies and meta-analyses. *Trends in Ecology & Evolution*, 39(5):435–445, 2024.

L. J. Revell and D. C. Collar. Phylogenetic analysis of the evolutionary correlation using likelihood. *Evolution*, 63 (4):1090–1100, 2009.

L. J. Revell, L. J. Harmon, and D. C. Collar. Phylogenetic signal, evolutionary process, and rate. *Systematic biology*, 57(4):591–601, 2008.

J. E. Rodriguez, D. R. Williams, and P.-C. Bürkner. Heterogeneous heterogeneity by default: Testing categorical moderators in mixed-effects meta-analysis. *British Journal of Mathematical and Statistical Psychology*, 76(2): 402–433, 2023.

R. V. Rohlfs, P. Harrigan, and R. Nielsen. Modeling gene expression evolution with an extended ornstein–uhlenbeck process accounting for within-species variation. *Molecular biology and evolution*, 31(1):201–211, 2014.

P. Sae-Lim, A. Kause, M. Janhunen, H. Vehviläinen, H. Koskinen, B. Gjerde, M. Lillehammer, and H. A. Mulder. Genetic (co) variance of rainbow trout (oncorhynchus mykiss) body weight and its uniformity across production environments. *Genetics Selection Evolution*, 47:1–10, 2015.

D. Schluter. *The Ecology of Adaptive Radiation.* Oxford University Press, Oxford, UK, 2000.

F. H. Shaw, R. G. Shaw, G. S. Wilkinson, and M. Turelli. Changes in genetic variances and covariances: G whiz! *Evolution*, pages 1260–1267, 1995.

D. Silvestro, A. Kostikova, G. Litsios, P. B. Pearman, and N. Salamin. Measurement errors should always be incorporated in phylogenetic comparative analysis. *Methods in Ecology and Evolution*, 6(3):340–346, 2015.

S. C. Stearns. *The Evolution of Life Histories*. Oxford University Press, Oxford, UK, 1992.

J. A. Tobias, C. Sheard, A. L. Pigot, A. J. Devenish, J. Yang, F. Sayol, M. H. Neate-Clegg, N. Alioravainen, T. L. Weeks, R. A. Barber, et al. Avonet: morphological, ecological and geographical data for all birds. *Ecology Letters*, 25(3):581–597, 2022.

M. Turelli. Heritable genetic variation via mutation–selection balance: Lerch's zeta meets the abdominal bristle. *Theoretical Population Biology*, 25:138–193, 1984.

M. Turelli. Phenotypic evolution, constant covariances, and the maintenance of additive variance. *Evolution*, pages 1342–1347, 1988.

J. M. Ver Hoef and P. L. Boveng. Quasi-poisson vs. negative binomial regression: how should we model overdispersed count data? *Ecology*, 88(11):2766–2772, 2007.

G. P. Wagner and L. Altenberg. Perspective: Complex adaptations and the evolution of evolvability. *Evolution*, 50 (3):967–976, 1996. doi: 10.1111/j.1558-5646.1996.tb02339.x.

G. P. Wagner, J. P. Kenney-Hunt, M. Pavlicev, J. R. Peck, D. Waxman, and J. M. Cheverud. Pleiotropic scaling of gene effects and the "cost of complexity". *Nature*, 452:470–472, 2008.

D. R. Williams, J. E. Rodriguez, and P.-C. Bürkner. Putting variation into variance: modeling between-study heterogeneity in meta-analysis. *PsyArXiv*, 2021.